

The Toll pathway mediates Drosophila resilience to Aspergillus mycotoxins through specific Bomanins

Rui Xu, Yanyan Lou, Antonin Tidu, Philippe Bulet, Thorsten Heinekamp, Franck Martin, Axel Brakhage, Zi Li, Samuel Liégeois, Dominique Ferrandon

▶ **To cite this version:**

Rui Xu, Yanyan Lou, Antonin Tidu, Philippe Bulet, Thorsten Heinekamp, et al.. The Toll pathway mediates Drosophila resilience to Aspergillus mycotoxins through specific Bomanins. EMBO Reports, 2022, 10.15252/embr.202256036 . hal-03843744

HAL Id: hal-03843744
https://hal.science/hal-03843744

Submitted on 2 Dec 2022

HAL is a multi-disciplinary open access archive for the deposit and dissemination of scientific research documents, whether they are published or not. The documents may come from teaching and research institutions in France or abroad, or from public or private research centers.

L'archive ouverte pluridisciplinaire **HAL**, est destinée au dépôt et à la diffusion de documents scientifiques de niveau recherche, publiés ou non, émanant des établissements d'enseignement et de recherche français ou étrangers, des laboratoires publics ou privés.



Distributed under a Creative Commons Attribution - NonCommercial - NoDerivatives 4.0 International License

Article

TRANSPARENT PROCESS OPEN ACCESS

EMBO reports

The Toll pathway mediates *Drosophila* resilience to *Aspergillus* mycotoxins through specific Bomanins

Rui Xu[1,2,3,†], Yanyan Lou[1,2,3,†], Antonin Tidu[2,4], Philippe Bulet[5,6], Thorsten Heinekamp[7], Franck Martin[2,4], Axel Brakhage[7,8], Zi Li[1], Samuel Liégeois[1,2,3,*] & Dominique Ferrandon[1,2,3,**]

Abstract

Host defense against infections encompasses both resistance, which targets microorganisms for neutralization or elimination, and resilience/disease tolerance, which allows the host to withstand/tolerate pathogens and repair damages. In *Drosophila*, the Toll signaling pathway is thought to mediate resistance against fungal infections by regulating the secretion of antimicrobial peptides, potentially including Bomanins. We find that *Aspergillus fumigatus* kills *Drosophila* Toll pathway mutants without invasion because its dissemination is blocked by melanization, suggesting a role for Toll in host defense distinct from resistance. We report that mutants affecting the Toll pathway or the 55C *Bomanin* locus are susceptible to the injection of two *Aspergillus* mycotoxins, restrictocin and verruculogen. The vulnerability of 55C deletion mutants to these mycotoxins is rescued by the overexpression of Bomanins specific to each challenge. Mechanistically, flies in which *BomS6* is expressed in the nervous system exhibit an enhanced recovery from the tremors induced by injected verruculogen and display improved survival. Thus, innate immunity also protects the host against the action of microbial toxins through secreted peptides and thereby increases its resilience to infection.

Keywords *Drosophila melanogaster*; fumitremorgin/verruculogen; fungal infections; resilience/disease tolerance; restrictocin

Subject Categories Immunology; Microbiology, Virology & Host Pathogen Interaction; Signal Transduction

DOI 10.15252/embr.202256036 | Received 26 August 2022 | Revised 6 October 2022 | Accepted 14 October 2022

EMBO Reports (2022) e56036

Introduction

The outcome of an infection depends on the interactions between a host and a pathogen with its armory of multifarious virulence factors. In the case of fungal pathogens, several hundred potential virulence factors are known to be secreted (Gao *et al*, 2011; Lebrigand *et al*, 2016). The host confronts the invading microorganism through the multiple arms of its immune system. There are also varied strategies that counteract the effect of toxins and more generally withstand and repair damages inflicted directly by the pathogen or indirectly by the host through its own immune response (Medzhitov *et al*, 2012; Ferrandon, 2013; Soares *et al*, 2017). Fungal infections represent a widespread major health threat worldwide affecting more than 150 million patients and cause directly or indirectly at least one and a half million deaths each year (Bongomin *et al*, 2017; Rodrigues & Nosanchuk, 2020). Our current understanding of fungal infections relies on the study of the host's innate and adaptive immune responses and in parallel on investigations of fungal virulence factors (Scharf *et al*, 2014; van de Veerdonk *et al*, 2017). *Aspergillus fumigatus* can synthesize and secrete a vast array of toxins and secondary metabolites, the *in vivo* functions of which are just starting to be deciphered (Frisvad *et al*, 2009; Macheleidt *et al*, 2016; Raffa & Keller, 2019). Whereas some fungal virulence factors allow *A. fumigatus* to elude detection by the immune system, a few mycotoxins such as gliotoxin or fumagillin are known to interfere with immune signaling and help neutralize immune cell functions (Cramer *et al*, 2006; Kupfahl *et al*, 2006; Konig *et al*, 2019). However, it is currently poorly known whether the innate immune system is able to detect and counteract the actions of mycotoxins through specific effectors.

Drosophila melanogaster represents a genetically amenable model system that is well-suited to study infections and innate immunity as there is no vertebrate-like adaptive immunity. Its innate immune system comprises several arms: a cellular response mediated by plasmatocytes in the adult, melanization, which depends on the cleavage of prophenol oxidases by Hayan, and the humoral systemic immune

1 Sino-French Hoffmann Institute, Guangzhou Medical University, Guangzhou, China
2 Université de Strasbourg, Strasbourg, France
3 Modèles Insectes de l'Immunité Innée, UPR 9022 du CNRS, Strasbourg, France
4 Architecture et Réactivité de l'ARN, UPR 9002 du CNRS, Strasbourg, France
5 CR Université Grenoble Alpes, Institute for Advanced Biosciences, Inserm U1209, CNRS UMR 5309, Grenoble, France
6 Platform BioPark Archamps, Archamps, France
7 Department of Molecular and Applied Microbiology, Leibniz Institute for Natural Product Research and Infection Biology - Hans Knöll Institute (Leibniz-HKI), Jena, Germany
8 Institute of Microbiology, Friedrich Schiller University Jena, Jena, Germany
*Corresponding author. Tel: +33 388417107; E-mail: s.liegeois@unistra.fr
**Corresponding author. Tel: +33 388417017; E-mail: d.ferrandon@ibmc-cnrs.unistra.fr
†These authors contributed equally to this work

© 2022 The Authors. Published under the terms of the CC BY NC ND 4.0 license.

14693178, 0, Downloaded from https://www.embopress.org/doi/10.15252/embr.202256036 by Cochrane France, Wiley Online Library on [02/12/2022]. See the Terms and Conditions (https://onlinelibrary.wiley.com/terms-and-conditions) on Wiley Online Library for rules of use; OA articles are governed by the applicable Creative Commons License

response (Lemaitre & Hoffmann, 2007; Liegeois & Ferrandon, 2022). A landmark study published 25 years ago established the central role of the Toll pathway in mediating the humoral immune response against fungal infections, as represented by *A. fumigatus* (Lemaitre *et al*, 1996). This observation has since been extended to a variety of other filamentous fungi or pathogenic yeast infections and also to several Gram-positive bacterial infections. The current paradigm is that upon sensing infections, a MyD88 adaptor-dependent intracellular signaling pathway gets activated by the binding of the processed Spätzle cytokine to the Toll receptor and stimulating the transcription of effector genes (such as antimicrobial peptides (AMPs)) that mediate its role in host defense. Genes encoding antifungal peptides such as Drosomycin, Metchnikowin, and Daisho are Toll-regulated AMPs active on filamentous fungi (Fehlbaum *et al*, 1995; Levashina *et al*, 1995; Cohen *et al*, 2020). However, in contrast to the other NF-κB signaling pathway that mediates host defense against Gram-negative bacteria, Immune deficiency (IMD), it is less clear whether Toll-dependent AMPs provide the bulk of the protection against Gram-positive or fungal infections. Indeed, the deletion of a locus encoding ten Toll-dependent secreted peptides at the 55C locus known as Bomanins largely phenocopies the *Toll* mutant phenotype (Uttenweiler-Joseph *et al*, 1998; Clemmons *et al*, 2015). This suggests that these peptides are somehow involved in mediating the defenses resulting from Toll pathway activation, which regulates the expression of more than 150 immune-responsive genes (De Gregorio *et al*, 2002). A majority of Bomanins at the 55C locus are short (BomS), the secreted form of which essentially contains a single domain characteristic of this family of peptides. Other members include a tail after the Bomanin domain (BomT) whereas bicipital members are characterized by the inclusion of two domains separated by a linker domain (BomBc). Although a recent study suggests that some BomS are likely active against *Candida glabrata* and can function somewhat redundantly (Lindsay *et al*, 2018), the exact function of most Bomanins in host defense remains uncertain.

How exactly *Drosophila* host defense confronts *A. fumigatus* and fungal virulence factors in general remains unknown despite our knowledge of the generic role of the Toll pathway in antifungal defense. Here, we revisit *A. fumigatus* infections obtained by injecting a limited number of conidia into the thorax and find that the fungus is unable to invade flies, including Toll pathway *MyD88* mutants, due to melanization, a distinct host defense, which is mediated by the Hayan protease and the PPO2 phenol oxidase. Our data suggest that Toll pathway immuno-deficient flies succumb to *A. fumigatus* secreted toxins, some of which target the nervous system. We report here that Toll mediates resilience to particular mycotoxins through specific Bomanins that do not function as classical AMPs in this setting but neutralize the effects of these fungal virulence factors. Our data illustrate that evolution has selected a specialized defense partially mediated by secreted peptides that allow the host to elude or counteract the action or effects of the attack by mycotoxins.

Results

Defense against *A. fumigatus* depends on the Toll pathway independently of its role in controlling AMP expression

Homozygous or hemizygous *MyD88* but not wild-type flies were highly sensitive to an *A. fumigatus* challenge with various strains and succumbed to as few as five injected conidia (Figs 1A and EV1A–C). Mutations in the *Drosophila* Toll pathway genes *spätzle* (*spz*) and *Toll* (*Tl*) led to an *A. fumigatus* susceptibility phenotype similar to that of *MyD88* (Fig EV1D and E).

Unexpectedly and in contrast to other relevant microbial infections in Toll pathway mutants (Alarco *et al*, 2004; Apidianakis *et al*, 2004; Quintin *et al*, 2013; Duneau *et al*, 2017), the fungal burden did not reach values higher than 200–300 colony-forming units (cfus) in *MyD88* flies challenged with 50 conidia (Fig 1B) or even upon the injection of 5,000 conidia (Fig EV1F). The lack of growth of *A. fumigatus* in *MyD88* flies was confirmed by measuring the fungal load upon death (FLUD; Fig EV1G). Monitoring a GFP-expressing *A. fumigatus* strain revealed the formation of mycelia only next to the injection site of 50 conidia in both wild-type and *MyD88* flies (Figs 1C and D, and EV1H). Puzzlingly, the injection of a higher number of conidia led to the formation of fewer hyphae (Fig EV1I). To exclude the possibility that death might be caused by another microorganism, possibly deriving from the microbiota, we confirmed the sensitivity of *MyD88* mutant flies to *A. fumigatus* challenge on antibiotics-treated flies and on axenic flies (Fig EV1J–L). We conclude that *MyD88* flies succumb to a low *A. fumigatus* burden (lower than 200 *A. fumigatus* cfus at death; Fig EV1G).

A septic injury with the Gram-positive bacterium *Micrococcus luteus* induces the expression of *Drosomycin* and all 55C *Bomanin* genes, *BomS4*-excepted (Fig EV2A and B). In contrast, the injection of even high doses of live or killed conidia did not induce the expression of *Drosomycin* steady-state transcripts measured by conventional RT–qPCR (Fig 1E). Only a mild induction of *Drosomycin* and the small secreted peptide-encoding gene *BomS1* were detected using digital PCR (RT–dPCR) in wild-type flies challenged with 5,000 conidia (Fig EV2C and D), which was confirmed by mass spectrometry detection of the induction of some BomS peptides but not Drosomycin in collected hemolymph (Fig EV2E and F, Appendix Fig S1). *Aspergillus fumigatus* infection thus induces weakly at the transcriptional level the expression of classical Toll pathway activation read-outs such as *BomS1* or *Drosomycin*. Surprisingly, only the short Bomanins and one Daisho peptide (DIM4) were reliably detected in the hemolymph via MALDI-TOF mass spectrometry. Their levels in the hemolymph were rather independent of the size of the inoculum (Fig EV2G), in keeping with the relatively stable fungal load measured (Fig EV1F). The expression of these peptides in the hemolymph tended to actually decrease upon injection of an inoculum > 1,000 conidia, possibly correlating with the decreased formation of hyphae and likely higher levels of gliotoxin.

Thus, the SPZ/Toll/MyD88 cassette is required for host defense against *A. fumigatus* infections, even though this pathogen only mildly stimulates the Toll pathway. Strikingly, the major read-out of the Toll pathway *Drosomycin* steady-state transcript levels and its encoded peptide, are only weakly induced.

Drosophila melanization curbs *A. fumigatus* invasion

As melanization is a host defense of insects effective against fungal infections, we tested *Hayan* mutant flies defective for this arm of innate immunity (Nam *et al*, 2012). These mutant flies were sensitive to *A. fumigatus* infection but less susceptible than *MyD88* mutant flies (Fig 1F). In contrast to *MyD88*, the fungal burden was

© 2022 The Authors

14693178, 0, Downloaded from https://www.embopress.org/doi/10.15252/embr.202256036 by Cochrane France, Wiley Online Library on [02/12/2022]. See the Terms and Conditions (https://onlinelibrary.wiley.com/terms-and-conditions) on Wiley Online Library for rules of use; OA articles are governed by the applicable Creative Commons License

increased in these mutants (Fig 1G and H). Further, the melanization response was dependent on Prophenoloxidase 2 (PPO2) but not PPO1 nor on the Sp7 protease (Fig EV3A–D). Thus, in contrast to a previous study that demonstrated a role for PPO1 and Sp7 in the host defense against low inocula of *Enterococcus faecalis* (Dudzic *et al*, 2019), it appears that a relevant melanization response downstream of Hayan can be mediated through PPO2, which like PPO1 is cleaved by Hayan (Nam *et al*, 2012). Interestingly, *A. fumigatus* disseminated throughout the body in *Hayan* mutants but was restricted to the thorax in *MyD88* flies (Fig EV3E). In keeping with these results, the fungus erupted in cadavers from all three tagmata, including the legs, of *Hayan* mutants (Fig 1I). In contrast, the fungus

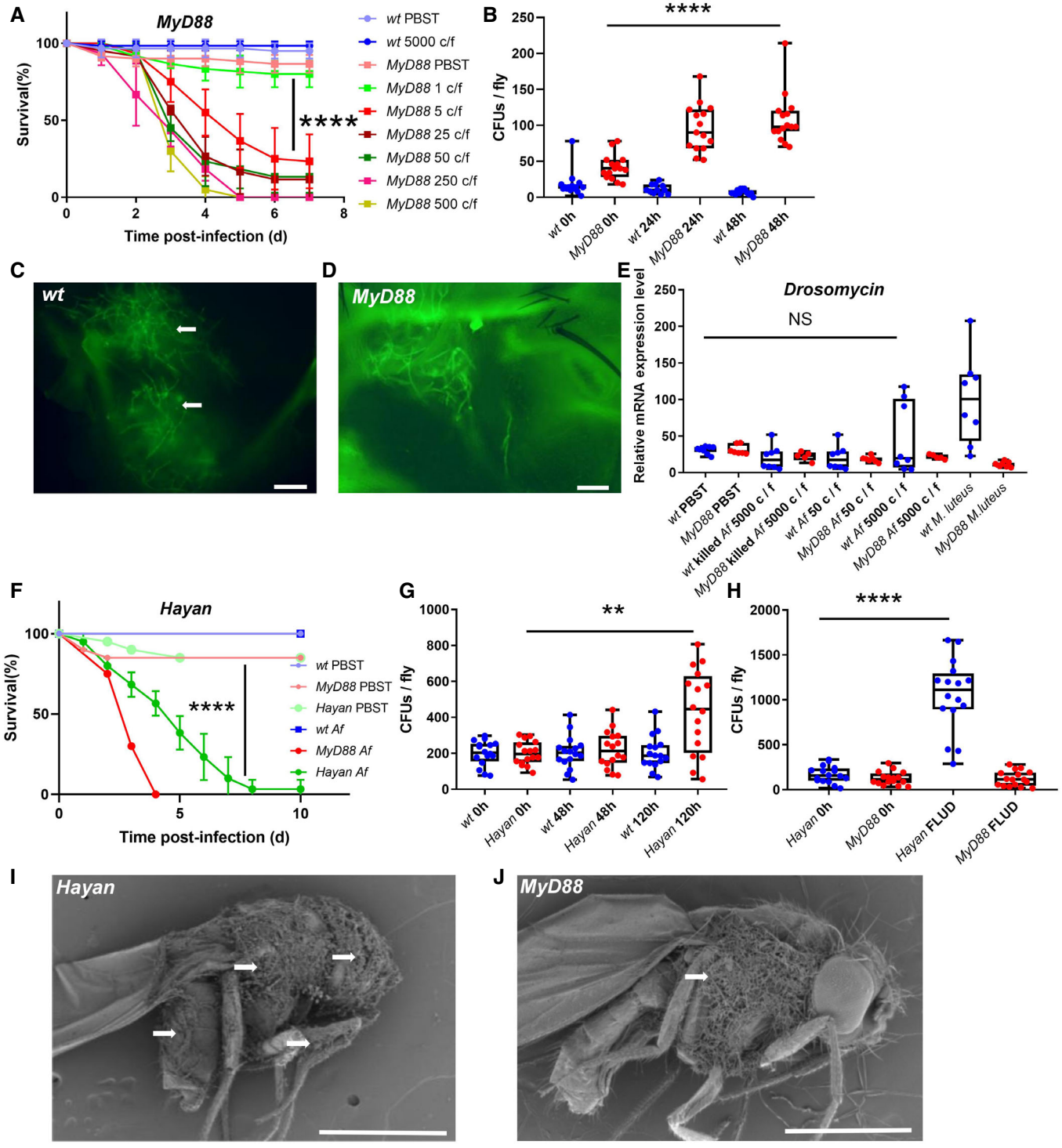


Figure 1.

14693178, 0, Downloaded from https://www.embopress.org/doi/10.15252/embr.202256036 by Cochrane France, Wiley Online Library on [02/12/2022]. See the Terms and Conditions (https://onlinelibrary.wiley.com/terms-and-conditions) on Wiley Online Library for rules of use; OA articles are governed by the applicable Creative Commons License

Figure 1. Toll pathway mutants succumb to *Aspergillus fumigatus* infection even though it is not required to limit the proliferation and dissemination of the pathogen, an immune function mediated by melanization.

A Survival curves of *MyD88* flies injected with different doses of *A. fumigatus* conidia (c/f: conidia injected per fly; error bars represent mean ± SD of the survival of biological triplicates of 20 flies each).

B Fungal loads of single *MyD88* mutant and wild-type flies (50 conidia injected per fly).

C, D GFP-labeled *A. fumigatus* (50 conidia per fly) injected in wild-type (C) or *MyD88* mutant (D) flies form hyphae in the thorax of the flies (arrows). Scale bars 50 μm.

E Expression level of *Drosomycin* induced by different doses of injected *A. fumigatus* conidia measured by RT–qPCR; *M. luteus* (OD = 10) represents the positive control (pooled data of $n = 3$ experiments, biological replicates).

F–H *Hayan* flies are susceptible to *A. fumigatus*. Survival (F), time course of fungal loads of single *Hayan* mutant flies (500 conidia per fly) (G), and fungal load upon death (500 conidia per fly) (H) of *Hayan* mutant flies; *Hayan* 0 versus 120 h, (error bars represent mean ± SD of the survival of biological triplicates of 20 flies each).

I, J *A. fumigatus* hyphae extrusion (arrows) from *Hayan* (I) and *MyD88* (J) mutant cadavers; scanning electron micrographs. Scale bars 750 μm.

Data information: In (B, E, G, H), the middle bar of box plots represents the median and the upper and lower limits of boxes indicate, respectively, the first and third quartiles; the whiskers define the minima and maxima; data were analyzed using the Mann–Whitney statistical test. Survival curves were analyzed using the log-rank test. $^{**}P = 0.004$; $^{****}P < 0.0001$, and NS: not significant.

only broke through the cuticle in the thorax where it had been injected in *MyD88*, *Toll* or *spz* mutants (Figs 1J and EV3F). Of note, the fungus did not erupt from infected wild-type flies killed mechanically. We conclude that melanization limits the proliferation and the dissemination of *A. fumigatus* injected into wild-type flies yet does not eradicate it at the injection site, where a melanization plug forms.

We also tested the contribution of the cellular immune response either by challenging *eater* mutant flies lacking a major phagocytosis receptor, presaturating the phagocytic apparatus by injection of latex beads, or by genetically ablating hemocytes. In each case, no enhanced sensitivity to *A. fumigatus* infection was observed (Appendix Fig S2A–C).

A. fumigatus secondary metabolism is required for its virulence in *Drosophila*

The finding that *A. fumigatus* killed *MyD88* immuno-deficient flies with a low fungal burden and limited dissemination in conjunction with the observation of the modest induction of the Toll pathway suggested that Toll pathway mutants could be sensitive to some of the many diffusible mycotoxins known to be secreted by this fungus (Frisvad *et al*, 2009). We first tested this hypothesis using an *A. fumigatus* mutant strain lacking the phosphopantetheinyl transferase (*pptA*) gene required for the biosynthesis of all secondary metabolites, including most mycotoxins (Johns *et al*, 2017). This *A. fumigatus* mutant strain was not virulent when its conidia were injected into *MyD88* flies (Fig 2A); its fungal burden was somewhat reduced after 48 h (Fig 2B). Importantly, the Δ*pptA* mutant managed to form a limited mycelium at the injection site (Fig 2C and D). These findings indicated that one or several mycotoxins are responsible for the observed phenotypes. However, gliotoxin was not required to kill *MyD88* mutant flies as a gliotoxin deletion mutant, *ΔgliP*, was still as virulent as wild-type *A. fumigatus* (Fig 2E). As expected from the analysis of the gliotoxin mutant strain, the injection of commercially-available gliotoxin killed wild-type and *MyD88* flies at a similar rate, but only when injected at sufficiently high concentrations (Fig 2F). By contrast, other antimicrobial compounds secreted by *A. fumigatus* (Raffa & Keller, 2019), namely fumagillin and helvolic acid, did not kill wild-type or *MyD88* flies at the tested concentrations (Fig 2G and H).

The Toll pathway is required in the host defense against some *A. fumigatus* tremorgenic mycotoxins

The *ftm* gene cluster of *A. fumigatus* is involved in the biosynthesis of secondary metabolites belonging to the tremorgenic toxins such as the fumitremorgins and verruculogen. The *ftmA* gene encodes the first enzyme of this biosynthetic pathway (Kato *et al*, 2013). As shown in Fig 3A, a *ΔftmA* mutant was slightly but reproducibly less virulent than the *ΔakuB* genetic background control strain, which is deficient for the nonhomologous end-joining DNA repair pathway. Whereas *MyD88* and wild-type flies behaved similarly after the injection of either low or high doses of verruculogen, *MyD88* flies were more sensitive than wild-type to this toxin injected at a 1 or 5 mg/ml concentration (or introduced as a powder thereby bypassing the need for dissolution in a DMSO-containing solvent), in conventional or microbe-free conditions (Figs 3B–D and EV4A). *Toll* and *spz* mutant flies also succumbed to injected verruculogen (Fig EV4B and C). *MyD88* flies were also sensitive to fumitremorgin C injected at concentrations greater than or equal to 1 mg/ml (Fig 3E).

Most wild-type and *MyD88* flies injected with verruculogen exhibited seizures as early as half an hour after injection and by 3 h all flies suffered from tremors (Fig 3F and Movies EV1–EV4). Interestingly, wild-type flies started recovering from seizures after verruculogen injection from 15 h onward; all surviving flies had recovered after about a day whereas *MyD88* flies never recovered (Fig EV4D). Of note, when challenging directly with verruculogen powder, *MyD88* flies did recover, but slower, likely because in this mode a lower effective dose of the mycotoxin is delivered (Fig EV4E). Upon closer inspection, we found that *MyD88*, but not wild-type flies, exhibited tremors after 2 days of *A. fumigatus* infection (Movie EV5). The Toll pathway is constitutively activated in $Toll^{10B}$ flies. As expected, $Toll^{10B}$ flies survived verruculogen injection like wild-type flies (Fig 3G). Remarkably, about 50% of these flies did not exhibit tremors at 3 h postinjection of verruculogen (Fig 3H). These data indicate that wild-type flies undergo the tremorgenic action of verruculogen and, in contrast to *MyD88* flies, are able to overcome the effects of the toxin in a resilience process that involves *spz*, *Toll*, and *MyD88*. Melanization and hemocytes did not appear to be involved in resilience to verruculogen action (Fig EV4F–H).

© 2022 The Authors

14693178, 0, Downloaded from https://www.embopress.org/doi/10.15252/embr.202256036 by Cochrane France, Wiley Online Library on [02/12/2022]. See the Terms and Conditions (https://onlinelibrary.wiley.com/terms-and-conditions) on Wiley Online Library for rules of use; OA articles are governed by the applicable Creative Commons License

The Toll pathway is required in the host defense against a ribotoxin

We next tested the contribution of another mycotoxin, restrictocin, a ribotoxin protein secreted by *A. fumigatus* and other pathogenic fungi. Restrictocin cleaves 28S ribosomal RNA and thereby inhibits host cell translation (Fando *et al*, 1985; Lamy *et al*, 1991; Nayak *et al*, 2001). Injection of *A. fumigatus* Δ*aspf1* conidia, which lack the restrictocin biosynthesis locus, resulted in a modest but reproducible reduction in virulence as compared to the *ΔakuB* genetic background control strain when injected into *MyD88* mutants (Fig 4A). Strikingly, the injection of restrictocin killed *MyD88* but not wild-type flies in untreated, antibiotics-treated or axenic flies (Fig 4B–D). Whereas the injection of restrictocin led to the demise

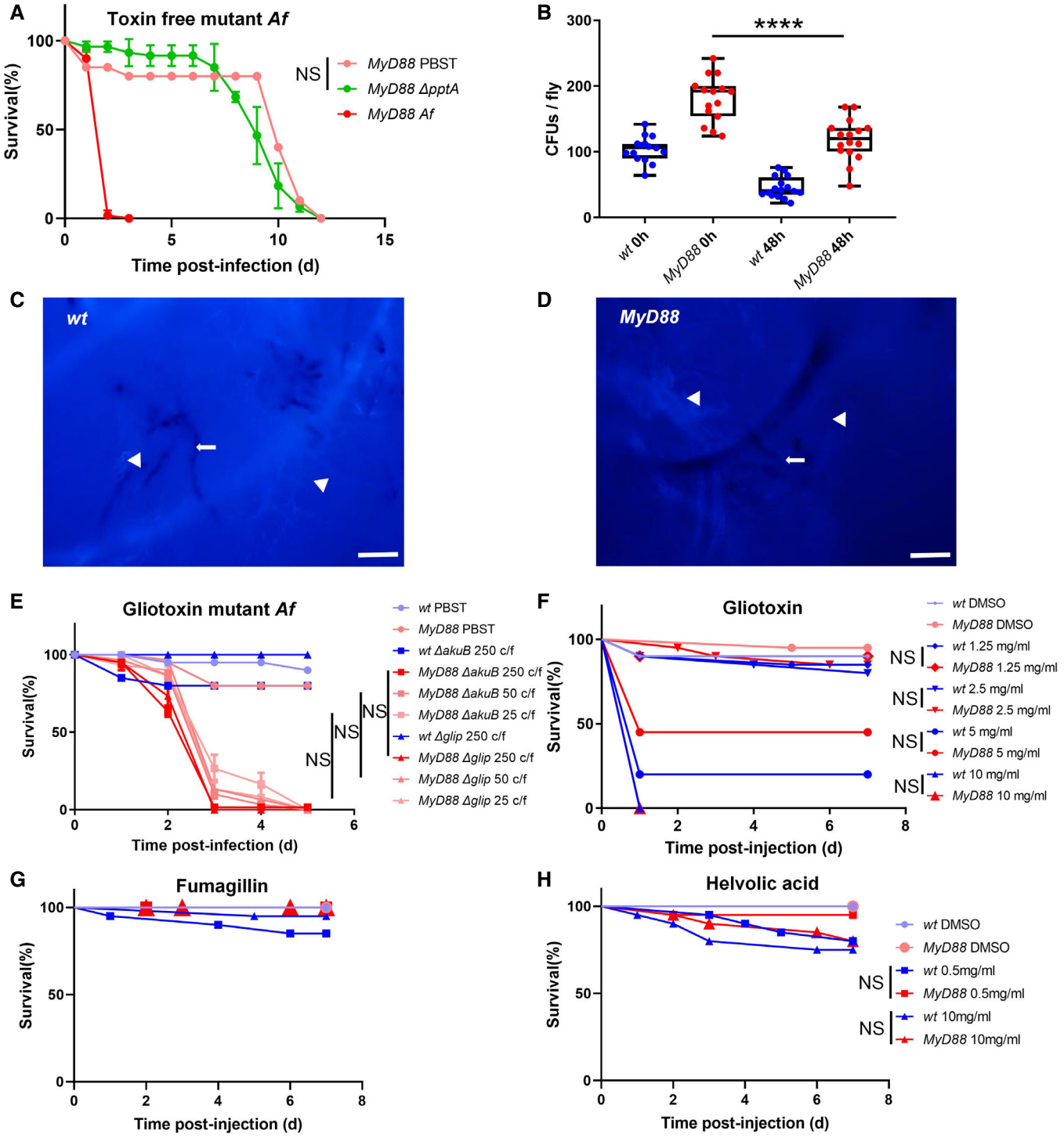


Figure 2.

© 2022 The Authors

14693178, 0, Downloaded from https://www.embopress.org/doi/10.15252/embr.202256036 by Cochrane France, Wiley Online Library on [02/12/2022]. See the Terms and Conditions (https://onlinelibrary.wiley.com/terms-and-conditions) on Wiley Online Library for rules of use; OA articles are governed by the applicable Creative Commons License

Figure 2. Secondary metabolism is critical for the virulence of *Aspergillus fumigatus* in *Drosophila MyD88* immuno-deficient flies.

A Survival of *MyD88* flies injected with *ΔpptA* and wild-type (*Af*) *A. fumigatus* conidia (error bars represent mean ± SD of the survival of biological triplicates of 20 flies each).

B Fungal loads of single flies after the injection of 500 *ΔpptA* conidia.

C, D Hyphae of *ΔpptA A. fumigatus* observed in the thorax of wild-type and *MyD88* flies (arrow) after Uvitex-B negative staining, air sacs and tracheae are stained by Uvitex-B (arrowheads). Scale bars 50 μm.

E Dose response of *MyD88* flies after *ΔgliP* (gliotoxin) mutant or wild-type [*ΔakuB*] *A. fumigatus* infection; error bars represent mean ± SD of the survival of biological triplicates of 20 flies each; wild-type flies are used as a control for the dose of 250 conidia.

F–H Dose response of *MyD88* and wild-type flies after gliotoxin (F), fumagillin (G), and helvolic acid (H) injection at the indicated concentrations (20 flies per condition).

Data Information: In (B), the middle bar of box plots represents the median and the upper and lower limits of boxes indicate, respectively, the first and third quartiles; the whiskers define the minima and maxima; data were analyzed using the Mann–Whitney test. Survival curves were analyzed using the log-rank test. ****$P < 0.0001$, and NS: not significant.

of *spz* and *Toll* mutant flies, it did not impact flies deficient for either melanization or the cellular immune response (Fig EV4I–M).

The cleavage by restrictocin of the 28S RNA between G_{4325} and A_{4326} yields a fragment of about 500 nucleotides known as the α-sarcin fragment (Gluck *et al*, 1994). When we analyzed total RNA extracted from *MyD88* restrictocin-injected flies, we observed a fragment of the expected size, which was not detected in PBS-injected flies. The α-sarcin peak was also detected upon the injection of restrictocin in wild-type flies. The cleavage of the 28S RNA was, however, much less pronounced in wild-type flies as compared to *MyD88* (Fig 4E and F). These observations suggest that the MyD88-mediated response is able to counteract restrictocin *in vivo* prior to its action on rRNA. In agreement with these results, the GFP fluorescence emitted from a transgene-induced ubiquitously at the time of the challenge was reduced 42 h after restrictocin injection. In addition, GFP fluorescence was lower upon *A. fumigatus* challenge than upon a mock infection (Fig 4G). Taken together, these data suggest that restrictocin is able to inhibit translation to a detectable degree *in vivo*, likely through the cleavage of the ribosomal 28S α-sarcin/ricin loop as described *in vitro*.

We therefore checked in a rabbit reticulocyte translation assay that restrictocin is blocking translation *in vitro* (Fig 4H), as previously reported (Nayak *et al*, 2001). This observation was extended to *Drosophila* S2 cell extracts. Since the Toll pathway cannot be induced in regular S2 cells, we used a stable line that expresses a chimeric Toll receptor (ERTL) that can be activated by adding Epidermal Growth Factor (EGF) to the growth medium (Sun *et al*, 2004). In extracts from noninduced cells, eGFP *in vitro* translation was inhibited by the addition of restrictocin in a dose-dependent manner (Appendix Fig S3A and B). Even though the Toll pathway was indeed activated by the addition of EGF, translation with an extract made from induced ERTL-S2 cells was nevertheless inhibited by the addition of restrictocin almost as efficiently as with an extract made from noninduced ERTL-S2 cells (Fig 4I and J). Thus, the Toll pathway may not act at the intracellular level but possibly through secreted effectors as detailed further below.

The Spätzle/Toll/MyD88 cassette is thus required for host defense against both verruculogen, a secondary metabolite, and restrictocin, a protein ribotoxin.

Bomanins mediate resilience to mycotoxins

The Toll pathway regulates the expression of at least 150 genes, including some Bomanins initially identified as *Drosophila* immune-induced molecules (Uttenweiler-Joseph *et al*, 1998; De Gregorio *et al*, 2002). Strikingly, the deletion of the 55C locus (Fig EV2A) that spans 10 *Bomanin* genes yields a phenotype as strong as Toll pathway mutants in several infection models (Clemmons *et al*, 2015). In the case of *A. fumigatus*, we found the $Bom^{\Delta 55C}$ deletion mutant to be only somewhat less susceptible to this infection than *MyD88* flies (Fig 5A). The fungal burden remained low during and after the infection (Fig 5B, Appendix Fig S4A). Interestingly, the $Bom^{\Delta 55C}$ mutant was also sensitive to the injection of verruculogen and restrictocin (Fig 5C and D; green curve). Only 25% of $Bom^{\Delta 55C}$ flies versus more than 50% for isogenized wild-type survived verruculogen injection after day 1. In the case of restrictocin, $Bom^{\Delta 55C}$ flies succumbed to this challenge, which was not the case for control flies. To exclude the possibility of a nonspecific sensitivity of *MyD88* or of $Bom^{\Delta 55C}$ flies to stress, we submitted these mutant flies and their isogenized controls to a variety of stresses such as heat shock at 37°C or 29°C or the injection of salt solution or H_2O_2 (Appendix Fig S4B–E). The injection of 4.6 nl of 8% NaCl solution or of 2% H_2O_2 did not reveal a differential susceptibility of the immune-deficient flies to these challenges. In contrast, we did observe a mild susceptibility of *MyD88* but not of $Bom^{\Delta 55C}$ flies to a continuous exposure to 37°C. Similar results were obtained for an exposure to 29°C with *MyD88* flies displaying an enhanced sensitivity but only after 12–15 days, that is, much later than the usual time frame of our experiments (Figs 1A, 3B and 4B).

We attempted to identify the relevant 55C cluster genes involved in host defense against injected mycotoxins using a genetic rescue strategy in which we overexpressed single 55C locus *Bomanin* genes in the background of the $Bom^{\Delta 55C}$ deficiency. Overexpression of either *BomBc1*, *BomS3*, or *BomS6* provided a significant degree of protection (comparable to wild-type flies) against restrictocin whereas *BomS6* and, to a variable extent, *BomS1* protected $Bom^{\Delta 55C}$ mutant flies from verruculogen (Fig 5C and D). Of note, we still observed the induction of tremors in verruculogen-injected rescue flies.

To determine whether BomS3 interacts with restrictocin *in vitro*, we tested whether the preincubation of restrictocin with a BomS3 synthetic peptide would decrease the inhibition of translation in ERTL-S2 cells. As shown in Appendix Fig S3C and D, it was as inefficient as control synthetic BomS1 peptide in blocking the inhibition of translation mediated by restrictocin. Thus, BomS3 is unlikely to act directly and independently against restrictocin and might act extracellularly.

As monitored by RT–dPCR, the expression of *BomBc1*, *BomS1*, and especially *BomS3* was induced by an *A. fumigatus* challenge

© 2022 The Authors

14693178, 0, Downloaded from https://www.embopress.org/doi/10.15252/embr.202256036 by Cochrane France, Wiley Online Library on [02/12/2022]. See the Terms and Conditions (https://onlinelibrary.wiley.com/terms-and-conditions) on Wiley Online Library for rules of use; OA articles are governed by the applicable Creative Commons License

(Figs 5E and F, and EV2D). Some other *Bom* genes located in 55C also exhibited a weak nonsignificant induction (Appendix Fig S5). As the injection of vehicle alone induced a significant response of some 55C locus genes, it was not possible to determine whether verruculogen is also able to induce their expression in this experimental series. We did find that the expressions of *BomBc1*, *BomS3*, and *BomS4* were induced to a low level by the injection of restrictocin (Fig 5E and F, Appendix Fig S5C), which was not the case for other *Bomanin* genes (Appendix Fig S5A, B and D–H).

BomS6 can protect flies from the toxic effects of verruculogen when expressed in the brain

That the ubiquitous overexpression of Tl^{10B} protects 50% of wild-type flies from the tremorgenic effects of verruculogen provided a convenient method to investigate which tissues mediate this effect. When we expressed the Tl^{10B} transgene in neurons, there was also a dominant protection of 50% of the flies from the tremors measured 3 h after the injection of verruculogen, an effect similar to its

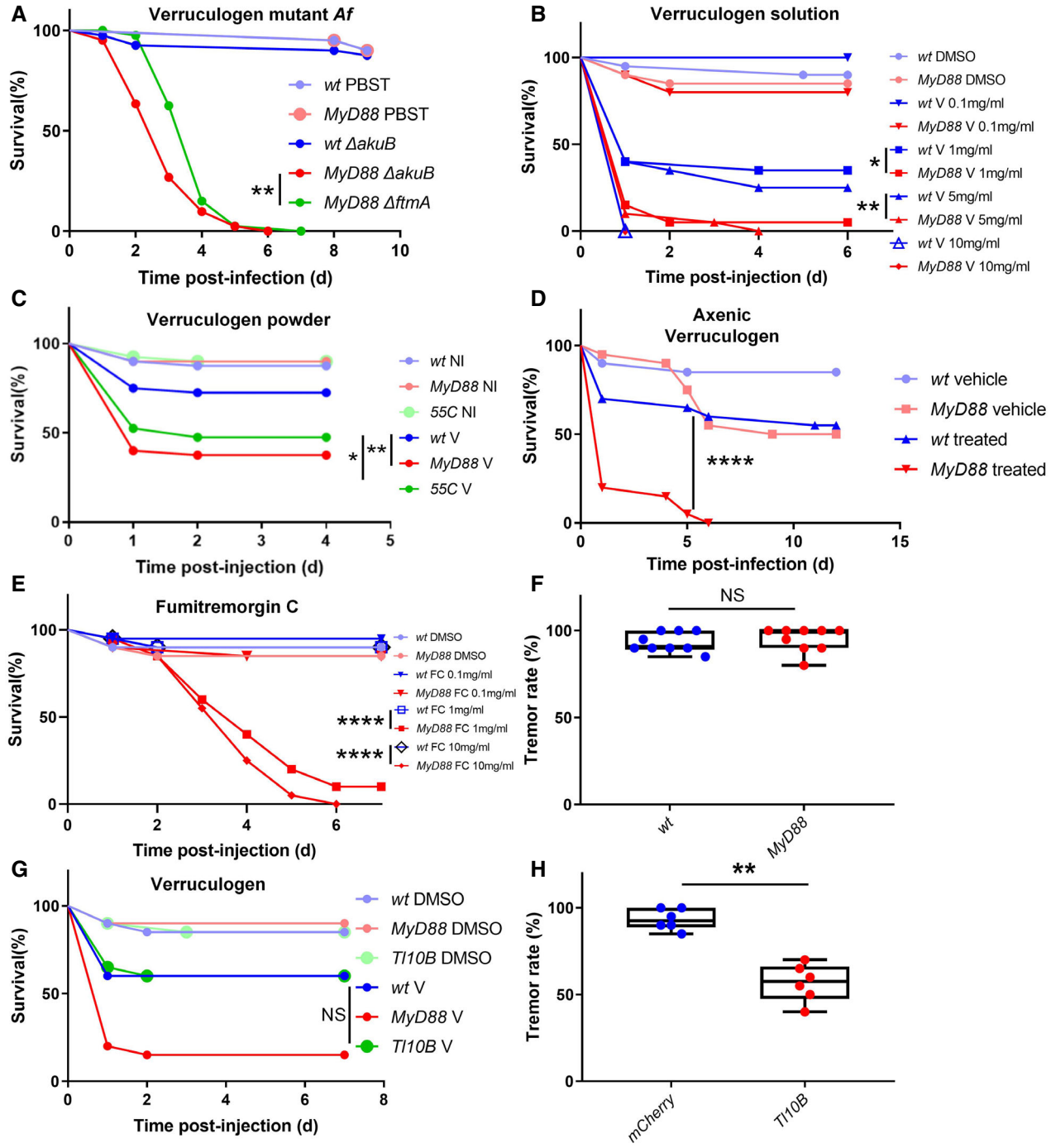


Figure 3.

14693178, 0, Downloaded from https://www.embopress.org/doi/10.15252/embr.202256036 by Cochrane France, Wiley Online Library on [02/12/2022]. See the Terms and Conditions (https://onlinelibrary.wiley.com/terms-and-conditions) on Wiley Online Library for rules of use; OA articles are governed by the applicable Creative Commons License

Figure 3. The Toll pathway mediates *Drosophila* resilience to *Aspergillus fumigatus* tremorgenic secondary metabolites of the fumitremorgin/verruculogen biosynthesis pathway.

A, B Survival of *MyD88* or wild-type flies after injection of 250 conidia of *ΔftmA* (verruculogen and fumitremorgins biosynthesis pathway mutant) or wild-type [*ΔakuB*] *A. fumigatus* (A) or verruculogen (V) (B) (20 flies per condition); *ΔakuB* versus *ΔftmA*, $^{**}P = 0.002$ (A); wt vs. *MyD88* (1 mg/ml verruculogen, $^{*}P = 0.015$; 5 mg/ml, $^{**}P = 0.008$ (B)).

C, D Survival of *MyD88* mutant flies after verruculogen powder challenge (C), and axenic *MyD88* mutant flies after verruculogen solution injection (D); wt V versus *55C* V, $^{*}P = 0.02$, versus *MyD88* V, $^{**}P = 0.002$ for verruculogen powder challenge (20 flies per condition).

E Survival of *MyD88* mutant flies after fumitremorgin C injection at different concentrations (20 flies per condition).

F Each dot corresponds to the tremor rate measured in a batch of 20 wild-type or *MyD88* flies 3 h after verruculogen injection (biological replicates).

G *Ubi-Gal4 > UAS-Toll^{10B}* flies survive like wild-type flies to verruculogen injection (20 flies per condition).

H Rate of *Ubi-Gal4 > UAS-Toll^{10B}* flies exhibiting tremors 3 h after injection of verruculogen in batches of 20 flies, each dot representing one batch; $^{**}P = 0.002$ (pooled data of $n = 3$ experiments, biological replicates).

Data Information: In (F, H), the middle bar of box plots represents the median and the upper and lower limits of boxes indicate, respectively, the first and third quartiles; the whiskers define the minima and maxima, and data were analyzed using the Mann–Whitney test. Survival curves were analyzed using the log-rank test. $^{****}P < 0.0001$, and NS: not significant. Except indicated otherwise (B), the concentration of injected verruculogen was 1 mg/ml.

ubiquitous expression (Figs 3H and 6A). We have shown above that 40% of flies in which *Tl^{10B}* was expressed ubiquitously succumbed to verruculogen injection, like wild-type flies (Fig 3G). In contrast, full protection was conferred to flies in which *Tl^{10B}* was expressed only in neurons (Fig 6B), which survived much better than wild-type flies. Similar observations were made when *Tl^{10B}* was expressed in glial cells, except that the degree of protection was weaker. This may reflect a side-effect of the overexpression strategy with a gene, the product of which is secreted: a cell type located in the vicinity of the physiologically relevant target cell type may partially achieve a biological activity (Fig 6C and D). We next tested the ectopic expression in a wild-type background of *BomS6*, which is the only peptide gene we found to reliably rescue the sensitivity phenotype of *Bom$^{\Delta 55C}$* flies in survival experiments after a verruculogen challenge. When *BomS6* was ectopically expressed in the nervous system, all of the flies displayed tremors 3 h after injection and there was no enhanced protection of this phenotype (Fig EV5A and B). However, when we measured the time it took for those flies to recover from tremors, we did find that they recovered faster, at a pace similar to that obtained by its ubiquitous ectopic expression (Fig 6E and F). Interestingly, flies in which *BomS6* was expressed in neurons or ubiquitously were fully protected against the noxious effects of verruculogen in survival experiments (Fig 6G). When *BomS6* was expressed in glial cells, the improved recovery from verruculogen challenge was nearly significant (Fig 6H, $P = 0.058$) and flies did survive significantly better than wild-type flies but nevertheless were less protected than when *BomS6* was expressed in neurons (Fig 6I). When we tried to repeat the experiment by ectopically expressing *BomS4*, no protection was conferred to those flies suggesting a degree of specificity of the *BomS* genes (Fig EV5C and D).

To determine whether *Bomanins* can be induced by mycotoxins, we monitored their expression by dRT–PCR on head samples after verruculogen powder challenge or restrictocin injection. Strikingly, we found that only the expression of *BomS6* and *BomS4* was increased by the verruculogen powder challenge (Fig 6J and K, Appendix Fig S6A–H). Unexpectedly, these two genes were also the only ones to be induced in the head by the injection of restrictocin (Fig 6L and M). In contrast, all 55C *Bomanin* genes were induced in the head after the injection of 500 *A. fumigatus* conidia, except for *BomS3* and *BomS4* (Fig 6L and M, Appendix Fig S7A–H). Of note, *Drosomycin* expression was induced in the head after an *A. fumigatus* challenge but not by restrictocin or verruculogen (Appendix Figs S6I and S7I). Thus, only two *Bomanin* genes are induced in the head in response to restrictocin or verruculogen injection.

Discussion

Here, we observed that *A. fumigatus* remains confined to its injection site in both wild-type and Toll pathway mutant flies due to the restriction of fungal dissemination by melanization, not annihilation. Thus, this rare occurrence of a localized infection together with the analysis of mycotoxin mutants of *A. fumigatus* confirms the fundamental role of mycotoxins in the virulence of *A. fumigatus* and reveals an unanticipated role for the Toll pathway in the protection against various secreted poisonous molecules. In the course of evolution, host defense effectors able to effectively neutralize the action or effects of mycotoxins have been selected independently of classical xenobiotic detoxification pathways that protect the host through modification and elimination of the compounds.

Toll pathway mutants succumb directly to *A. fumigatus* or mycotoxin challenge

The microbiota plays an important role in various aspects of the biology of *Drosophila* (Lesperance & Broderick, 2020). Besides, bacteria, viruses may also participate in killing Toll pathway mutants as has been shown to be the case for ingested *Drosophila* C virus (Ferreira *et al*, 2014). As we did observe a significant lethality in some of our control experiments with the injection of PBS, especially on *MyD88* mutants, it was important to exclude the possibility of the microbiota playing a role in the observed susceptibility phenotypes by using either antibiotics treatment or axenic flies, which still succumbed to our experimental challenges; these experiments showed that the death of Toll pathway mutant flies is caused by the treatment and not an auxiliary infection. Of note, the antibiotics treatment was as effective as using axenic flies in suppressing the lethality observed sometimes in PBS-injected flies, which suggests that some bacteria escape from the digestive tract upon injury of the exoskeleton.

Induction of the expression of specific *Bomanin* genes upon mycotoxin challenge

The induction of *Drosomycin* transcripts by injected *A. fumigatus* conidia appears at best to be very mild as compared to that

© 2022 The Authors

14693178, 0, Downloaded from https://www.embopress.org/doi/10.15252/embr.202256036 by Cochrane France, Wiley Online Library on [02/12/2022]. See the Terms and Conditions (https://onlinelibrary.wiley.com/terms-and-conditions) on Wiley Online Library for rules of use; OA articles are governed by the applicable Creative Commons License

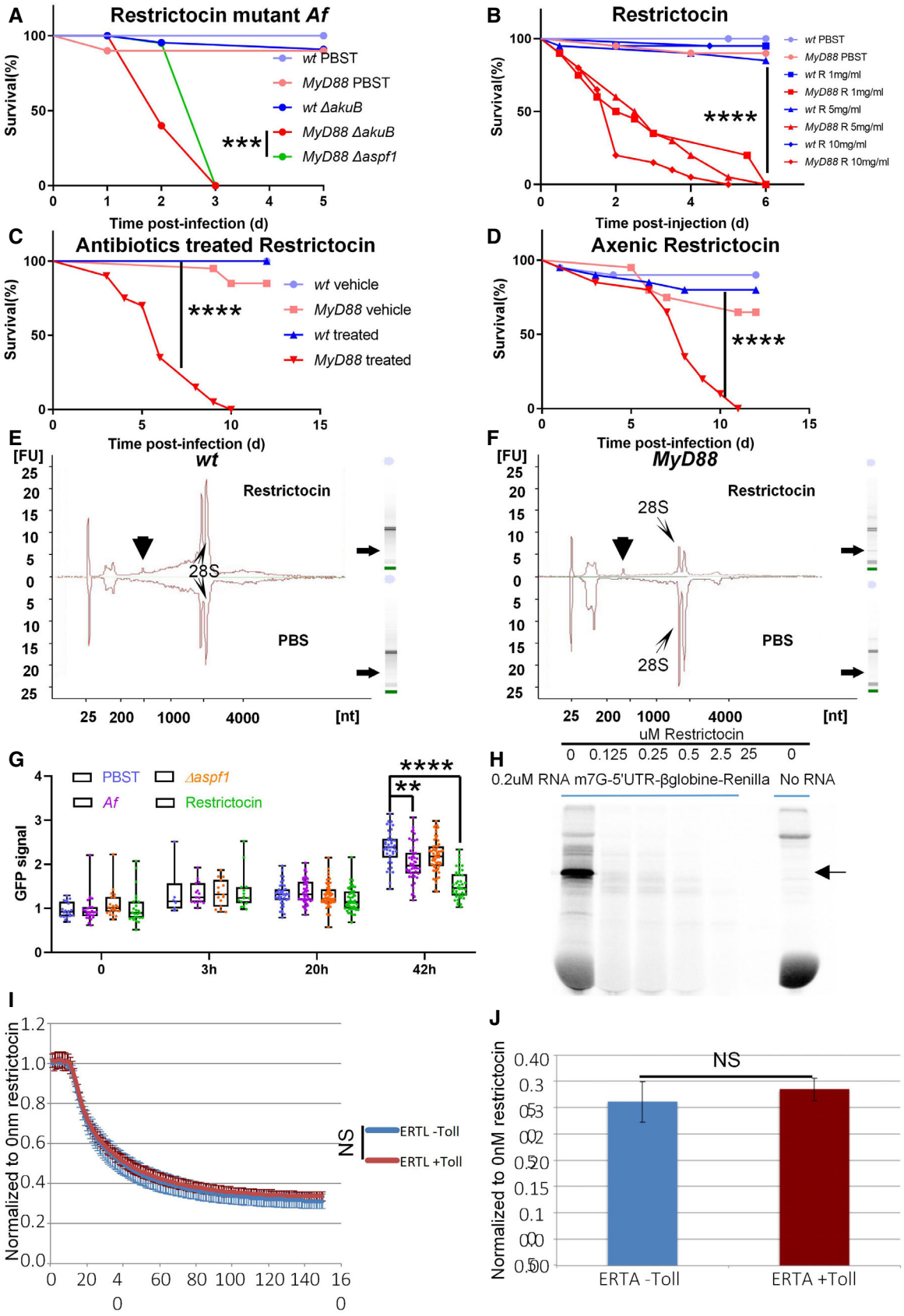


Figure 4.

14693178, 0, Downloaded from https://www.embopress.org/doi/10.15252/embr.202256036 by Cochrane France, Wiley Online Library on [02/12/2022]. See the Terms and Conditions (https://onlinelibrary.wiley.com/terms-and-conditions) on Wiley Online Library for rules of use; OA articles are governed by the applicable Creative Commons License

Figure 4. Restrictocin functions as a ribotoxin *in vitro* and *in vivo* and affects *MyD88* mutant and not wild-type flies.

A Survival of *MyD88* or wild-type flies to 250 injected *Δaspf1* (restrictocin mutant) or wild-type [*ΔakuB*] *A. fumigatus* conidia (20 flies per condition); *MyD88: Δaspf1* versus *ΔakuB* (***$P = 0.0007$).

B Survival of *MyD88* flies after the injection of different concentrations of restrictocin (R) (20 flies per condition).

C, D Survival of antibiotics-treated (C) and axenic (D) *MyD88* mutant flies after restrictocin injection (20 flies per condition).

E, F Ribosomal RNA cleavage measurement after restrictocin or PBS injection in wild-type (E) and *MyD88* (F) flies; the arrowheads show the position of the 28S RNA-derived α-sarcin fragments whereas arrows on the right show its electrophoretic band position.

G Fluorescence (arbitrary units) emitted by transgenic p*Ubi-Gal4-Gal80ts* > *UAS-GFP* whole flies induced at the same time as the challenge and measured at the indicated time points; PBST versus *Af*: **$P = 0.002$ (pooled data of $n = 3$ experiments, biological replicates).

H SDS–PAGE analysis of ^{35}S-labeled translated proteins produced in a rabbit reticulocytes lysate from a m^{7}G-capped reporter RNA containing the 5′UTR of β-globin followed by the Renilla luciferase coding sequence (arrow), in the presence of increasing concentrations (0.125–25 nM) of restrictocin.

I, J Fluorescence analysis from *in vitro* translated eGFP from an IGR (CrPV)-driven reporter in noninduced (blue) and Toll-induced (red) ERTL lysates: translation kinetics of *in vitro* synthesized eGFP in the presence of 1 nM restrictocin showing fluorescence values normalized to untreated translation reactions (I) and a histogram representing the end-point fluorescence quantification of I (J).

Data Information: In (G), the middle bar of box plots represents the median and the upper and lower limits of boxes indicate, respectively, the first and third quartiles; the whiskers define the minima and maxima; data were analyzed using the Kruskal–Wallis test and Dunn's *post hoc* test. In (I), error bars represent mean ± SEM ($n = 3$, technical replicates); in (J), error bars represent mean ± SEM ($n = 3$, technical replicates). Survival curves were analyzed using the log-rank test. ****$P < 0.0001$, and NS: not significant.

induced by the monomorphic yeasts *C. glabrata* or *Saccharomyces cerevisiae* that were easily detected by regular RT–qPCR (Quintin *et al*, 2013). This may be linked to the masking of ß-(1-3) glucans by hydrophobin proteins or melanin on the conidial cell wall (van de Veerdonk *et al*, 2017; Blango *et al*, 2019). The secretion of inhibitors of NF-κB signaling such as gliotoxin may also be at work (Pahl *et al*, 1996). It is, however, perplexing that secreted short Bomanins but not Drosomycin were detected by mass spectrometry in the hemolymph even though this peptide is massively produced during the systemic immune response to injected bacteria, at an estimated concentration of 0.3 μM (Uttenweiler-Joseph *et al*, 1998).

We find that the injection of restrictocin in flies leads to a modest yet significant induction of only a subset of *Bomanins*, *BomBc1*, *BomS3*, and *BomS4* (Fig 5E and F, Appendix Fig S5C). In contrast, all of them but *BomS4*—which has the lowest basal expression—are induced by a systemic immune challenge by *M. luteus* (Fig EV2B). Only *BomS4* and *BomS6* were induced in the head after the injection of verruculogen (Fig 6J and K, Appendix Fig S6A–H). This differential expression of *Bomanin* genes upon mycotoxin injection, especially that of *BomS4* that is not induced in the systemic immune response, suggests that the observed induction is not due to peptidoglycan contaminating the mycotoxin preparations as it would have induced almost all *Bomanins*. Of note, we have likely employed higher concentrations of mycotoxins than actually released during infection. Indeed, whereas *BomS4* is induced in heads by verruculogen powder challenge, it is not induced there after *A. fumigatus* infection. Taken together, these data then suggest that a process akin to the immune surveillance of core cellular processes first described in *Caenorhabditis elegans* may also exist in *Drosophila*. For instance, toxins that affect the translation machinery lead to the induction of varied host defenses, a situation similar to that encountered with restrictocin that indirectly inhibits translation by targeting the ribosomal 28S RNA (Dunbar *et al*, 2012; McEwan *et al*, 2012; Melo & Ruvkun, 2012). We conclude that restrictocin and verruculogen induce a response limited to two *BomS* genes in the head, which is distinct from that induced in the framework of the Toll-dependent systemic immune response.

Functions and specificity of Bomanins encoded at the 55C locus

The current paradigm for insect immune-induced secreted peptides is that they primarily represent AMPs (Hanson & Lemaitre, 2020; Lazzaro *et al*, 2020; Lin *et al*, 2020). This has been checked experimentally by the deletion of multiple AMP genes loci; the deletion of AMP genes regulated mostly by the IMD pathway phenocopied the susceptibility to Gram-negative bacteria of IMD pathway mutants (Hanson *et al*, 2019). This was, however, less clear as regards the deletion of AMP genes regulated by the Toll pathway. It appears that 55C locus *Bomanin* genes play a predominant role in the host defense against Gram-positive bacteria, yeasts, and fungi (Clemmons *et al*, 2015; Hanson *et al*, 2019). It is clear that some of these genes are required in the resistance against *E. faecalis*, suggesting that some Bomanins may function as AMPs (Clemmons *et al*, 2015). *Bom^{Δ55C}* deficiency flies are susceptible to *C. glabrata* infection and this susceptibility was rescued by overexpressing *BomS* genes such as *BomS3* (Lindsay *et al*, 2018). However, no *C. glabrata* killing activity of synthetic Bom peptides could be found in *in vitro* assays (Lindsay *et al*, 2018), even though hemolymph collected from wild-type but not mutant flies was fungicidal. The lack of fungicidal activity in the hemolymph of *Bom^{Δ55C}* flies was partially restored in the hemolymph of *Bom^{Δ55C}* mutant flies overexpressing *BomS5*, suggesting that at least this peptide may have some candicidal activity when combined with other Toll-dependent gene product(s) (Lindsay *et al*, 2018). While that study suggested that BomS peptides are interchangeable against *C. glabrata* provided they are expressed at sufficiently high levels, we report here that the BomS peptides appear to be much more specific with respect to the activity against mycotoxin action. Indeed, in the setting of the *Bom^{Δ55C}* deficiency, only overexpressed BomS6 or BomS1 show some activity against verruculogen, whereas the forced expression of BomS6, BomS3, or BomBc1 appears to be able to counteract restrictocin. An antimicrobial role has been proposed for BomS3 against *C. glabrata* by Lindsay *et al* (2018). It cannot be, however, formally excluded that BomS3 might also act against an unidentified *C. glabrata* secreted toxin. In this respect, it has recently been reported that *C. glabrata* is able to invade the brain (Benmimoun *et al*, 2020) where we suspect that the activation of the Toll pathway signaling is also taking place.

© 2022 The Authors

14693178, 0, Downloaded from https://www.embopress.org/doi/10.15252/embr.202256036 by Cochrane France, Wiley Online Library on [02/12/2022]. See the Terms and Conditions (https://onlinelibrary.wiley.com/terms-and-conditions) on Wiley Online Library for rules of use; OA articles are governed by the applicable Creative Commons License

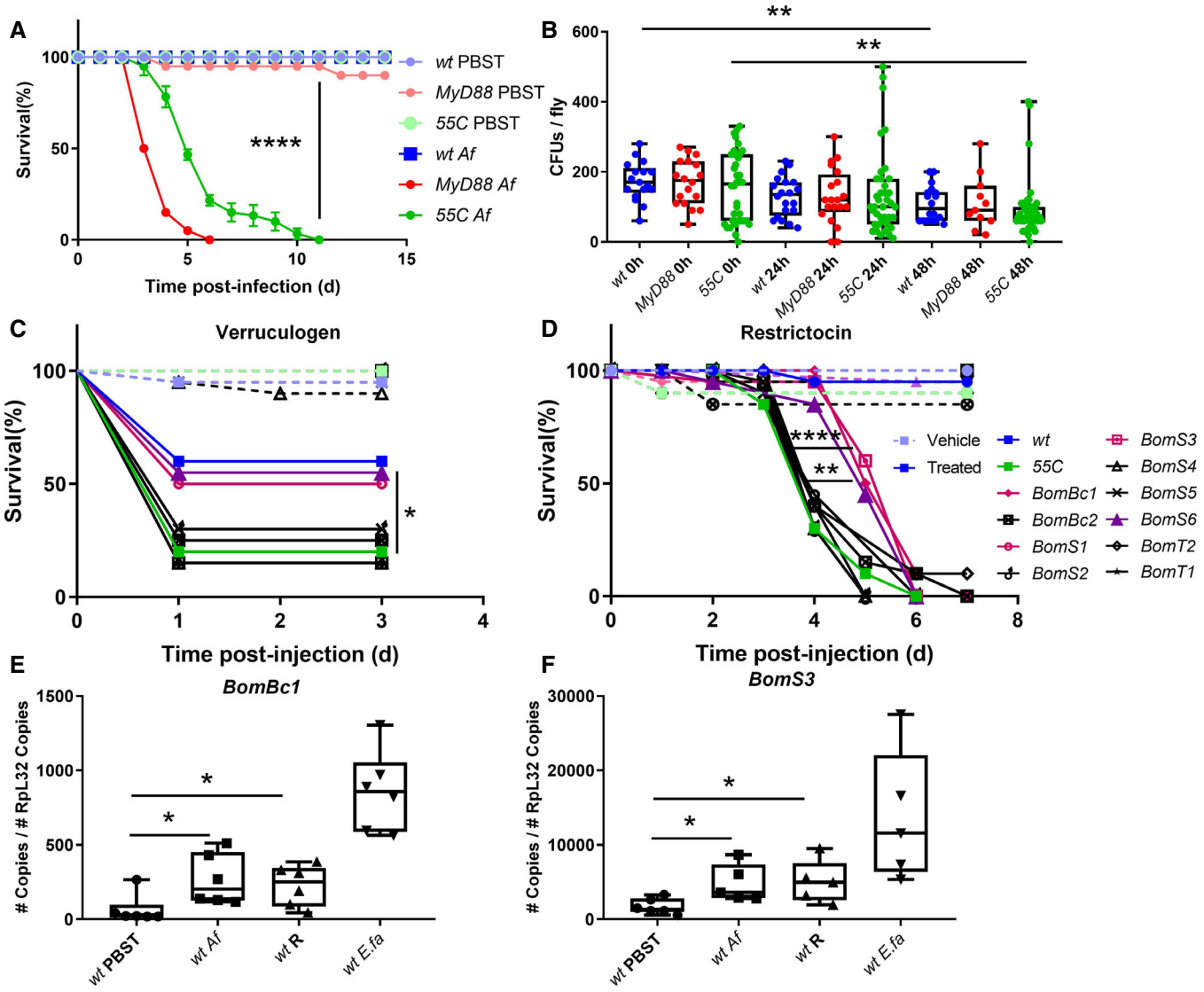


Figure 5. Distinct *Bomanins* mediate resilience to specific *Aspergillus fumigatus* mycotoxins.

A, B Survival (A) and fungal load (B) of $Bom^{\Delta 55C}$ (55C) deficient flies compared with wild-type and *MyD88 flies* after injection of 250 conidia (error bars represent mean ± SD of the survival of biological triplicates of 20 flies each); ****$P < 0.0001$. (B) The fungal burden does not increase in $Bom^{\Delta 55C}$-deficient flies; wt 0 versus 48 h, **$P = 0.001$; 55C 0 versus 48 h, **$P = 0.007$; pooled data of $n = 3$ experiments, biological replicates.

C, D Rescue of the sensitivity of $Bom^{\Delta 55C}$ flies to verruculogen (C) or to restrictocin (D) by the transgenic expression of individual 55C locus genes (caption in D also applies to (C)). 55C flies versus *BomS1*, *$P = 0.0495$, versus *BomS6* *$P = 0.011$ for verruculogen assay (C); 55C flies versus *BomBc1* or *BomS3*, ****$P < 0.0001$, 55C flies versus *BomS6*, **$P = 0.0028$ for restrictocin assay (D) (20 flies per condition).

E, F Expression levels of *BomBc1*, and *BomS3* measured by RT–digital PCR 48 h after challenge; *BomBc1* PBST versus *Af*, *$P = 0.015$, PBST versus restrictocin (R), *$P = 0.015$; *BomS3*: PBST versus *Af*, *$P = 0.02$, PBST versus R, *$P = 0.03$ (pooled data of $n = 3$ experiments, biological replicates).

Data Information: In (B, E, F), the middle bar of box plots represents the median and the upper and lower limits of boxes indicate, respectively, the first and third quartiles; the whiskers define the minima and maxima; data were analyzed using the Mann–Whitney statistical test. Survival curves were analyzed using the log-rank test.

With respect to host defense against restrictocin, our partial rescue data of the $Bom^{\Delta 55C}$ susceptibility phenotype by three 55C *Bomanins*, including one encoding a bicipital Bomanin might be accounted for by some form of redundancy. We cannot, however, exclude that these Bomanins provide a degree of protection through separate mechanisms, especially since the two Bomanin domains of Bc1 are rather divergent when compared to the high degree of conservation exhibited by BomS domains (Clemmons *et al*, 2015). Yet, *BomS6* is the sole 55C *Bomanin* providing protection against both restrictocin and verruculogen. BomS6 contains a lysine residue at position 10 of its Bomanin domain, like BomS2 but unlike BomS4 that contains a valine whereas other BomS peptides have an arginine at this position. The other difference is an isoleucine instead of valine at position 14 of the Bomanin domain. Thus, these

© 2022 The Authors

14693178, 0, Downloaded from https://www.embopress.org/doi/10.15252/embr.202256036 by Cochrane France, Wiley Online Library on [02/12/2022]. See the Terms and Conditions (https://onlinelibrary.wiley.com/terms-and-conditions) on Wiley Online Library for rules of use; OA articles are governed by the applicable Creative Commons License

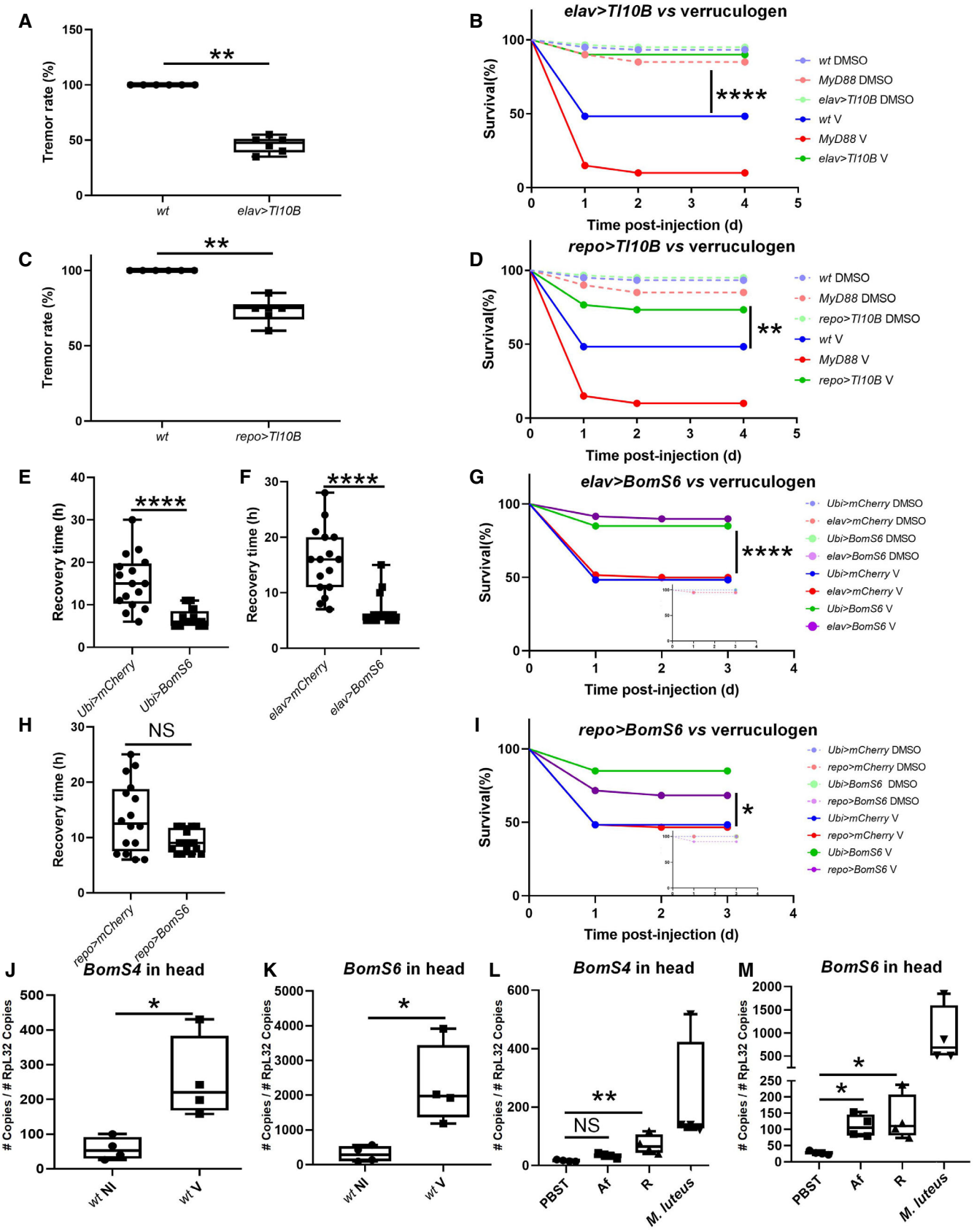


Figure 6

© 2022 The Authors

14693178, 0, Downloaded from https://www.embopress.org/doi/10.15252/embr.202256036 by Cochrane France, Wiley Online Library on [02/12/2022]. See the Terms and Conditions (https://onlinelibrary.wiley.com/terms-and-conditions) on Wiley Online Library for rules of use; OA articles are governed by the applicable Creative Commons License

Figure 6. *Bomanin S6* mediates resilience to verruculogen in the nervous system of *Drosophila*.

A, B Tremor rate (A) and survival (B) of flies (20 flies per condition) overexpressing *Tl[10B]* in neurons compared with wild-type after injection of verruculogen. (A) Each dot corresponds to the tremor rate measured in a batch of 20 flies; tremor rate *wt* versus *elav* > *UAS-Toll*^{10B}, $^{**}P = 0.002$.

C, D Tremor rate (C) and survival (D) of flies (20 flies per condition) overexpressing *Tl[10B]* in glia compared with wild-type after injection of verruculogen. (C) Each dot corresponds to the tremor rate measured in a batch of 20 flies; tremor rate *wt* versus *repo* > *UAS-Toll*^{10B}, $^{**}P = 0.002$. (D) Survival *wt* V versus *repo* > *UAS-Toll*^{10B} V, $^{**}P = 0.005$.

E–G Recovery time from tremor (E, F) and survival (G) of single flies overexpressing *BomS6* ubiquitously (E, G) or in neurons (F, G) (biological replicates) compared with wild-type after injection of verruculogen; in (G) the inset represents the survival of vehicle control groups.

H, I Recovery time from tremor (H) and survival (I) of single flies overexpressing *BomS6* in glia (pooled data from $n = 3$ experiments, biological replicates) compared with wild-type after injection of verruculogen; in (I) the inset represents the survival of vehicle control groups. Recovery time (H) *repo* > *mCherry* versus *repo* > *BomS6*, $P = 0.058$, survival (I) *repo* > *mCherry* V versus *repo* > *BomS6* V, $^{*}P = 0.016$.

J–M Expression of *BomS4* (J) and *BomS6* (K) in the head after verruculogen powder challenge, and *BomS4* (L) and *BomS6* (M) in the head after *A. fumigatus* (*Af*), restrictocin or *M. luteus* injection (pooled data from $n = 3$ experiments, biological replicates).

Data Information: In (A, C, E, F, H, J–M), the middle bar of box plots represents the median and the upper and lower limits of boxes indicate, respectively, the first and third quartiles; the whiskers define the minima and maxima; data were analyzed using the Mann–Whitney statistical test. Survival curves were analyzed using the log-rank test. $^{*}P < 0.05$, $^{**}P < 0.01$, $^{****}P < 0.0001$, and NS: not significant. In this figure, the concentration of injected verruculogen or restrictocin was 1 mg/ml.

biochemical differences along the capacity to be induced in the heads by *A. fumigatus* and verruculogen account for the unique function of BomS6 among Bomanins.

Whereas we propose here a specific function for some Bomanins in counteracting the effects of restrictocin or verruculogen, we cannot formally exclude an AMP function in other contexts. Indeed, it has previously been reported that mammalian alpha-defensin AMPs are also able to directly neutralize secreted bacterial virulence factors such as pore-forming toxins or enzymes that need to penetrate inside eukaryotic cells to act on their intracellular target (Kudryashova *et al*, 2014 and references therein). These proteins are inherently thermodynamically unstable as they need to change their conformations to insert or go through the mammalian cell plasma membrane. The amphipathic properties of alpha-defensins allow them to destructure these secreted virulence factors through hydrophobic interactions and thereby inactivate them (Kudryashova *et al*, 2014). Such a mechanism might be at play as regards a potential interaction of Bomanins with restrictocin, which does cross the plasma membrane. Indeed, the N-terminal part of mature BomS6 appears to be rather hydrophobic (38% of residues are hydrophobic) and uncharged. As regards verruculogen, it acts through hydrophobic interactions with one of its molecular targets (see further below), and possibly, BomS6 might also directly interact with verruculogen through hydrophobic interactions, although other BomS peptides (e.g., BomS3) exhibit similar or higher hydrophobicity.

The mechanism of action of restrictocin in inhibiting translation is well established and it crosses the plasma membrane of insects easily. Thus, it may act ubiquitously on all cell types and organs of the host. Wild-type flies tolerate exposure to a relatively large range of restrictocin concentrations whereas *MyD88* flies succumb faster to a high dose of 10 mg/ml (Fig 4B); the Toll-dependent response to *A. fumigatus* is not dose-dependent (Fig EV2G). Toll in wild-type flies blocks to a large extent the action of restrictocin since it prevents the cleavage of 28S rRNA (Fig 4E and F). BomS3, however, does not appear to directly bind to restrictocin (Appendix Fig S3C and D). Taken together, these observations suggest an indirect mode of action of Bomanins, at least for BomS3 and BomS6.

Our understanding of the action(s) of verruculogen on the nervous system is less clear as multiple effects are reported in the literature. These include increased spontaneous release of glutamate and aspartate from cerebrocortical synaptosomes (Hotujac *et al*, 1976; Norris *et al*, 1980), inhibition of the $GABA_A$ receptor (Gant *et al*, 1987) or inhibition of calcium-activated K^+ channels (Knaus *et al*, 1994) such as *Drosophila* Slowpoke, for which a detailed structural understanding of its interaction with verruculogen is available (Raisch *et al*, 2021). In contrast to the effect of restrictocin, verruculogen induces tremors also in wild-type flies, but unlike *MyD88* flies, these are able to reverse this effect, a situation also observed in cattle (Norris *et al*, 1980; Gant *et al*, 1987). The constitutive activation of the Toll pathway neutralizes to a significant extent the tremorgenic effects of injected verruculogen early on. Interestingly, BomS6 appears to function somewhat differently when overexpressed in the nervous system of wild-type flies. It does not prevent the initial tremors induced by verruculogen but allows the host to recover more rapidly, which suggests that two distinct processes are at play. Thus, Tl^{10B} may function through an effector that is distinct from BomS6 in the early protection against tremors; alternatively, this other effector may act in concert with BomS6. Future studies should determine whether the actions of Bomanins are direct or indirect, the latter being more likely given the different targets of restrictocin, verruculogen, and fumitremorgins. One may wonder whether Bomanins might alter the permeability of the plasma membrane for instance. The recent finding of a role for another Toll pathway effector, BaramicinA, in glial cells against a neurotoxin opened the possibility of an indirect role of BaraA in regulating the permeability of the Blood–Brain-Barrier (preprint: Huang *et al*, 2022).

Perspectives

Our work presented here and in a concurring study suggests that host defense has evolved to select mechanisms not only to directly fight off invading microorganisms such as AMPs but also to protect the host against the toxins they secrete (preprint: Huang *et al*, 2022). The identification of specific effectors of *Drosophila* innate immune signaling pathways evolved to counteract toxins is an important addition to our emerging understanding of host strategies implemented to cope with such microbial weapons, e.g., pore-forming toxins, fungal toxins in the gut, alpha-defensins (Kudryashova *et al*, 2014; Greaney *et al*, 2015; Lee *et al*, 2016; Chikina *et al*, 2020). It will be interesting to determine whether innate immunity also protects at least to some extent against mycotoxins that contaminate the food that present a major health threat for animals and humans (Brown *et al*, 2021).

© 2022 The Authors

14693178, 0, Downloaded from https://www.embopress.org/doi/10.15252/embr.202256036 by Cochrane France, Wiley Online Library on [02/12/2022]. See the Terms and Conditions (https://onlinelibrary.wiley.com/terms-and-conditions) on Wiley Online Library for rules of use; OA articles are governed by the applicable Creative Commons License

Aspergillosis causes acute or chronic infections in an estimated 14 million patients (Kosmidis & Denning, 2015; Gago *et al*, 2019). Chronic infections represent major threats to the survival of patients with comorbidities. It will therefore be important to establish whether mammalian antifungal innate immune response pathways also contribute to resilience against mycotoxins as is the case for the Toll pathway in flies. Finally, our findings open the possibility of the existence of host defenses that protect immunocompetent animals or humans against some mycotoxins but leave individuals deficient for these defenses susceptible to disease.

Materials and Methods

Microbial strains

Aspergillus fumigatus was cultured on potato dextrose agar (PDA) medium supplemented with 0.1 g/l chloramphenicol in an incubator at 29°C. Conidia were harvested after 4–7 days of culture. The conidial suspension was purified by filtration on cheese cloth to eliminate hyphae and other impurities. The standard wild-type *A. fumigatus CEA17ΔakuB*^{Ku80} (CEA17) is a kind gift from Drs. Anne Beauvais and Jean-Paul Latge (Institut Pasteur, Paris) and is also the genetic background control for *ΔgliP*. Other wild-type strains include D141 (background for D141-GFP), Af293, ATCC46645, A1160 (background for *ΔpptA*), GFP-labeled strain (D141-GFP). *ΔpptA* (secondary metabolites free mutant) and *ΔgliP* (gliotoxin-free mutant) have been previously described (Hillmann *et al*, 2015; Johns *et al*, 2017).

For targeted deletion of *ftmA* (AFUB_086360) and *aspf1* (AFUB_050860) gene replacement cassettes were generated by three-fragment-based PCR as described previously (Szewczyk *et al*, 2006). In brief, deletion constructs were generated by amplifying around 1 kb up- and downstream sequences of the respective gene and insertion of the pyrithiamine resistance cassette (Kubodera *et al*, 2000) by fusion PCR. Protoplasts of *CEA17ΔakuB*^{Ku80} *A. fumigatus* strain (da Silva Ferreira *et al*, 2006) were transformed with purified PCR products. Transformants were selected for resistance to pyrithiamine. Homologous recombination and integration of the deletion cassette were validated by PCR. Phusion Flash High-Fidelity Master Mix (Thermo Scientific, Germany) was used for all reactions. *A. fumigatus* was cultivated in *Aspergillus* minimal medium (Jahn *et al*, 1997). Media were supplemented with 0.1 mg/l pyrithiamine (Merck, Germany) when required.

The sequence of primers is found in Appendix Table S1.

Micrococcus luteus CGMCC#1.2299 was cultured in Tryptic soy broth (TSB), and *E. faecalis* CGMCC#1.2135 was cultured in Luria-Bertani (LB) at 37°C for 24 h. The bacteria were then washed in PBS thrice and resuspended.

Fly strains

Fly lines were raised on food at 25°C with 65% humidity. For 25 l of fly food medium, 1.2 kg cornmeal (Priméal), 1.2 kg glucose (Tereos Syral), 1.5 kg yeast (Bio Springer), 90 g nipagin (VWR Chemicals) were diluted into 350 ml ethanol (Sigma-Aldrich), 120 g agar-agar (Sobigel) and water qsp were used.

w^{A5001} flies were used as wild-type control unless otherwise indicated. Canton-S (BDSC64349), w^{1118} (VDRC60000), and y^1w^1 were used as further wild-type controls as needed. The following mutant lines were used: *MyD88*^{c03881}, *Df (2R)3591*, *Hayan*^{34}, *w*, P{*ry*, *Dipt-LacZ*}, P{w^+, *drs-GFP*}; *spz*^{rm7}, *spz*^{u5}, *Toll*^{632}. The following strains *Df(3R)Tl-I*, *e*^{1}*/TM3*, *Ser*^{1} (BDSC1911), *eater*^{1}, *SP7*, *PPO1*$^{\Delta}$, and *PPO2*$^{\Delta}$ were kind gifts from Dr. Bruno Lemaitre; *eater*$^{\Delta}$ mutants were obtained by crossing the two deficiency lines *Df(3R)Tl-I*, *e*^{1}*/TM3*, *Ser*^{1} (BDSC1911) and *Df(3R)D605/TM3*, *Sb*^{1} *Ser*^{1} (BDSC823). *spz* and *Tl* mutants used in this study were either transheterozygous or hemizygous mutants crossed at 25°C. *phmlΔ*-Gal4 > UAS-eGFP is a reporter line for hemocytes, *w*, P{UAS-*rpr*.C}, P{UAS-*hid*} flies (a kind gift of Akira Goto) were crossed to the *phmlΔ-Gal4 > UAS-eGFP* line at 29°C to ablate hemocytes during development. *UAS-Toll*^{10B} flies were crossed to a *w*; *pUbi-Gal4*, *pTub-Gal80ts* (BDSC30140) or to *elav-Gal4* or *repo-Gal4* driver lines at 25°C; hatched adults were placed at 29°C for 5 days to activate the Toll pathway.

The *Bom*$^{\Delta 55C}$ deficiency was a kind gift of Steven Wasserman that was further isogenized in the w^{A5001} background. The transgenic lines expressing single *Bom* genes of the 55C locus under the *pUAS-hsp70* promoter control were generated as described (list of primers in Appendix Table S1) and checked by sequencing. The transgenic flies were crossed to a *w*; *pUbi-Gal4*, *pTub-Gal80*^{ts} driver line, in a homozygous *Bom*$^{\Delta 55C}$ mutant or w^{A5001} background. The expression of the transgenes was checked by RT–qPCR and mass spectrometry analysis on collected hemolymph of single flies as required.

Preparation of toxin or chemical stress solutions

Restrictocin (Sigma) was resuspended in phosphate buffer saline (PBS) pH = 7.2, gliotoxin (Abcam), helvolic acid (Abcam), fumagillin (Abcam), verruculogen (Abcam), fumitremorgin C (Sigma), were dissolved at 10 mg/ml in Dimethyl sulfoxide (DMSO; Molecular biology grade, Sigma) as stock solutions and stored at −20°C. A working concentration of 1 mg/ml in DMSO was used for injections of 4.6 nl of all toxin solutions unless otherwise indicated. Toxin solutions were thawed on ice for 1 h prior to use. As multiple freeze/thaw cycles reduce the potency of the toxins, care was taken not to use an aliquot more than five times and aliquots were not stored for more than 1 month. NaCl (Sigma) and 3% H_2O_2 solutions in PBS pH 7.2 were prepared freshly for each injection.

Axenic flies

To obtain axenic flies, eggs were collected, washed with water, and then 70% ethanol prior to dechorionation of eggs in a solution of 50% bleach until the chorion disappeared. Eggs were transferred into sterile vials containing media and a mix of antibiotics: ampicillin, chloramphenicol, erythromycin, and tetracycline. Once emerged, adult flies were crushed and tested on LB-, Brain-Heart infusion Broth-, MRS, and yeast peptone dextrose agar plates to observe any contamination by bacteria or fungi. Of note, no anaerobic microorganisms have been detected in the *Drosophila* microbiota.

Flies treated with antibiotics were fed on food containing ampicillin, tetracycline, chloramphenicol, erythromycin, and kanamycin at 50 μg/ml final concentration each. Females were collected after two generations on fly food with antibiotics and checked for sterility by plating.

© 2022 The Authors

14693178, 0, Downloaded from https://www.embopress.org/doi/10.15252/embr.202256036 by Cochrane France, Wiley Online Library on [02/12/2022]. See the Terms and Conditions (https://onlinelibrary.wiley.com/terms-and-conditions) on Wiley Online Library for rules of use; OA articles are governed by the applicable Creative Commons License

A. fumigatus infections and injection of toxins or chemical stress solutions

For *A. fumigatus* infections, spores were prepared freshly for each infection. Unless otherwise stated, spores were injected into the thorax (mesopleuron) of adult flies, usually at a concentration of 250–500 spores in 4.6 nl PBS containing 0.01% Tween20 (PBST) unless indicated otherwise, using a microcapillary connected to a Nanoject II Auto-Nanoliter Injector (Drummond). The same volume of PBS-0.01% Tween20 (PBST) was injected for control experiments. All experiments were performed at 29°C unless otherwise indicated. Prior to all infection experiments, the flies were incubated in tubes containing only 100 mM sucrose solution for 2 days to eliminate traces of antifungal preservatives added to the regular food. Toxins were injected as for *A. fumigatus* injection, except that a toxin or a chemical stress solution was used instead of a spore suspension. As noted, verruculogen powder was directly introduced into flies as follows: the ethanol-cleaned needles were not filled but just dipped into the powder and then used to prick the flies. The procedure was reiterated for each fly. Whereas the injected quantity is not determined with accuracy, it nevertheless yielded reproducible results, which were, however, weaker than when injecting verruculogen initially dissolved into DMSO. Flies were kept on regular food without preservatives after injection.

Saturation of phagocytosis

Latex bead injection was performed as previously described (Nehme *et al*, 2011; Quintin *et al*, 2013). The injected flies were placed on 100 mM sucrose solution for 48 h prior to injections.

Survival tests

Survival tests were usually performed using 5–7-day old flies. Twenty flies per vial in biological triplicates were maintained at 25°C. The transgenic overexpression flies were transferred from 18 to 29°C for 7 days before the challenge to allow the expression of Gal4, which is repressed by the $Gal80^{ts}$ repressor at 18°C. Surviving flies were counted every day. Each experiment shown is representative of at least three independent experiments unless indicated otherwise. For the heat stress experiments, flies were placed either at 29 or 37°C.

Quantification of the fungal load

The fungal burden was determined using single adult flies per condition. Single flies were transferred into arrays of 8 tubes (Starstedt) containing two 1.4-mm ceramic beads (Dominique Dutcher) in 100 µl PBS-0.01% Tween20. Single flies were homogenized by shaking using a mixer mill 300 or 400 (F. Kurt Retsch GmbH & Co. KG) at a frequency of 30/min twice for 30 s and plated on potato dextrose agar (PDA) plates supplemented with antibiotics. After that, the plates were enclosed with Parafilm™ and cultured at 29°C with 65% humidity. Colony-forming units were counted after 48 h. FLUD was performed as described (Duneau *et al*, 2017).

Monitoring of *A. fumigatus* infection *in vivo*

Flies were sacrificed and dissected in 8-well diagnostic microscope slides (Thermo Scientific; Carl Zeiss). was used for negative staining of *ΔpptA's* hyphae, by adding to each well 5 µl Uvitex-2B for 30 s at room temperature. Flies injected by D141-GFP or *ΔpptA* were dissected and observed under an epifluorescent Zeiss axioscope microscope (Carl Zeiss) each hour after the injection.

Preparation UV-killed *A. fumigatus*

The conidial suspension at about 10^{10} conidia/ml was plated on dried potato dextrose agar (PDA) supplemented with 0.1 g/l chloramphenicol plates and exposed twice for 3 h to the UV-light of a microbiology safety hood. Plates were cultured at 29°C with 65% humidity, after 48 h to check for the absence of colonies. The dead conidia were resuspended and counted prior to injection.

Scanning electron microscope

Whole flies were incubated in 1 ml of a solution of 0.1 M phosphate buffer pH 7.2, glutaraldehyde 2.5%, and paraformaldehyde 2.4% final at room temperature for at least 1 h. The flies were embedded in resin prior to observation with a scanning electron microscope (Hitachi S 800).

Drosomycin and *Bomanins* expression measurement

Expression of *Drosomycin* and *Bom* genes was measured by RT–qPCR and RT–digital PCR as described previously (Gottar *et al*, 2006; Madic *et al*, 2016). With respect to digital PCR, the results (# copies/µl) are normalized by the counts of the *Rpl32* reference gene from the same reverse-transcribed sample, as also done for regular RT–qPCR. The sequences of primers are shown in Appendix Table S1.

Restrictocin-mediated inhibition of translation

28S RNA α-sarcin fragment

Total RNA of restrictocin or PBS-injected flies was extracted using Trizol reagent on samples of 2–3 flies. Samples were loaded in the RNA 6000 Nano chip (Agilent RNA 6000 Nano, 2100 electrophoresis Bioanalyzer) to detect the peak corresponding to the α-sarcin fragment.

Level of protein synthesis inhibition in vivo

The level of inhibition of protein by injected restrictocin or the infection by *A. fumigatus in vivo* was assessed by measuring GFP fluorescence in single fly extracts. *w*; *pUbi-Gal4*, $ptub\text{-}Gal80^{ts}$ were crossed to *w*; *UAS-GFP* flies at 18°C. The progeny from the cross was kept at 18°C until *A. fumigatus* or restrictocin injection; the flies were then placed at 29°C thereafter and analyzed at the indicated times. Each fly was homogenized in 200 µl PBS solution prior to measuring the GFP fluorescence using a Varioskan 2000 fluorometer (Thermo Fisher Scientific).

Preparation of in vitro translation extracts from noninduced and Toll-induced ERTL cells

ERTL cells were grown for 5 days at 25°C in 25 ml of culture medium. For the Toll-induced ERTL cells, the culture medium was supplemented with 2.5 µg/ml recombinant mouse EGF (Sigma-Aldrich) 16 h before harvesting.

© 2022 The Authors

14693178, 0, Downloaded from https://www.embopress.org/doi/10.15252/embr.202256036 by Cochrane France, Wiley Online Library on [02/12/2022]. See the Terms and Conditions (https://onlinelibrary.wiley.com/terms-and-conditions) on Wiley Online Library for rules of use; OA articles are governed by the applicable Creative Commons License

After harvesting, cells were washed two times in cold 40 mM HEPES–KOH pH 8, 100 mM potassium acetate, 1 mM magnesium acetate, and 1 mM DTT solution, and resuspended at a concentration of 10^9 cells/ml in the same buffer supplemented with 1X Halt™ Protease Inhibitor Cocktail EDTA-free (Thermo Scientific™). Cell lysis was performed by nitrogen cavitation with a Cell Disruption Bomb (Parr Instrument Company). The lysate was cleared by centrifugations at 4°C with 10,000 *g*, aliquoted, frozen in liquid nitrogen, and stored at −80°C. The induction of the Toll pathway was checked by monitoring the transcript levels of *Drosomycin* by RT–qPCR.

In vitro translation assays in rabbit reticulocyte lysate and ERTL cell lysates

In vitro translation experiments in rabbit reticulocyte lysate were performed as previously described (Martin *et al*, 2011). *In vitro* translation experiments in ERTL cell lysates were performed as previously described for S2-cell lysates (Gross *et al*, 2017). eGFP *in vitro* translation was assessed by measuring fluorescence (λex = 485 nm; λem = 520 nm) every minute for 150 min.

Quantification of tremors and the recovery

Tremor quantification was performed after the injection of 4.6 nl of a 1 mg/ml verruculogen solution to batches of 20 w^{A5001} flies placed afterward in an empty vial. Biological triplicates were analyzed for each of the three independent experiments. The rate of tremor cases was measured in each tube 3 h after the injection. Tremor phenotypes are shown in videos available in the supplementary material of this article.

The tremor recovery was measured every 30 min: the flies that had recovered are the ones exhibiting no tremors and able to walk upwards on the sides of an empty vial. Observations were performed every 30 min and flies that had recovered (exhibiting no tremors and able to walk upwards on the sides of the vial) were removed. Three independent experiments were performed.

MALDI mass spectra analysis

MALDI spectra obtained from *Drosophila* hemolymph were acquired and analyzed using FlexControl and Flex Analysis (Bruker Daltonics) software or converted for analysis with the open-source mass spectrometry tool mMass (http://www.mmass.org). A sandwich sample preparation was used, which consists of deposition of (1) 0.5 µl of a saturated solution of 4HCCA in acetone, (2) 0.6 µl of acidified hemolymph in 0.1 µl of trifluoroacetic acid (TFA), and (3) 0.4 µl of a saturated solution of 4HCC in a solution of acetonitrile/0.1TFA (2:1). After a soft drying, spots were acquired in a linear positive mode at an attenuation maintained adjusted between 50 and 60 using a Bruker Daltonics UltraflexIII-Smartbeam instrument. Calibration of the measurements was made using the "DroCal" mixture containing the synthetic peptides BomS1, BomS2, BomS3, and BomS5 as well as a deuterated form of BomS1 (BomS1-ValD at 1,676.50 m/z with $z = 1$).

Quantification and statistical analysis

All statistical analyses were performed using Prism 7 or Prism 8 (GraphPad Software, San Diego, CA). The Mann–Whitney and/or Kruskal–Wallis tests were used unless otherwise indicated. The log-rank test was used to analyze survival experiments. When using parametric tests (analysis of variance (ANOVA) and *t*-test), a Gaussian distribution of data was checked using either D'Agostino-Pearson omnibus or Shapiro–Wilk normality tests. All experiments were performed at least three times, unless otherwise indicated. Significance values: $*P < 0.05$; $**P < 0.01$; $***P < 0.001$; $****P < 0.0001$.

Data availability

In this study, no primary datasets have been generated or deposited in external repositories.

Expanded View for this article is available online.

Acknowledgements

We thank Anne Beauvais and Jean-Paul Latge for the *A. fumigatus* strain used in this study, Won-Jae Lee, Bruno Lemaitre, Jiyong Liu, Steven Wasserman, Akira Goto, Angela Giangrande, and the Guangzhou Drosophila Resource Center for fly stocks. Stocks obtained from the Bloomington Drosophila Stock Center (NIH P40OD018537) were also used in this study. We gratefully acknowledge the contributions of Valérie Demais from Plateforme d'Imagerie *in vitro* (UPS 3156-Université de Strasbourg) for scanning electron microscopy, Sébastien Voisin from the BioPark for MALDI-TOF analysis, and Miriam Yamba for expert technical help. We thank Adrian Acker for the gift of the ERTL S2 cells, controls, and advice on the *in vitro* experimental conditions. Finally, we are indebted to Matthew Blango and Robert Unckless for critical reading of the manuscript. RX and YL were, respectively, partially funded through the Sino-Foreign cooperative graduate education project of Guangzhou Medical University and the International Training Plan for young outstanding scientific research talents of Guangdong Province. This work was supported by the Deutsche Forschungsgemeinschaft collaborative research center/transregion 124 FungiNet (project A1) and the excellence cluster Balance of the Microverse to TH and AB, the Association Platform BioPark of Archamps on its Research & Development budget (PB), by grants from "Agence Nationale pour la Recherche" (ANR-17-CE12-0025) to AT and FM, from the 111 Project (#D18010; China), the Incubation Project for Innovative Teams of the Guangzhou Medical University, the Open Project from State Key Laboratory of Respiratory Diseases, China, and the China High-end Foreign Talent Program to DF.

Author contributions

Rui Xu: Conceptualization; resources; formal analysis; validation; investigation; methodology; writing – original draft; writing – review and editing. **Yanyan Lou:** Conceptualization; resources; formal analysis; investigation; methodology; writing – original draft; writing – review and editing; performed and analyzed the mass spectrometry analysis. **Antonin Tidu:** Formal analysis; validation; investigation; methodology; writing – original draft; designed, performed and analyzed the *in vitro* translation experiments. **Philippe Bulet:** Resources; formal analysis; funding acquisition; validation; investigation; methodology; performed and analyzed the mass spectrometry analysis; generated the *A. fumigatus* mutants reported in this study. **Thorsten Heinekamp:** Resources; writing – original draft; generated the *A. fumigatus* mutants reported in this study. **Franck Martin:** Conceptualization; resources; supervision; funding acquisition; writing – original draft; designed, performed and analyzed the *in vitro* translation experiments. **Axel Brakhage:** Conceptualization; resources; funding

© 2022 The Authors

14693178, 0, Downloaded from https://www.embopress.org/doi/10.15252/embr.202256036 by Cochrane France, Wiley Online Library on [02/12/2022]. See the Terms and Conditions (https://onlinelibrary.wiley.com/terms-and-conditions) on Wiley Online Library for rules of use; OA articles are governed by the applicable Creative Commons License

acquisition; writing – original draft; writing – review and editing; generated the *A. fumigatus* mutants reported in this study. **Zi Li:** Conceptualization; resources; funding acquisition; project administration. **Samuel Liégeois:** Conceptualization; resources; formal analysis; supervision; validation; investigation; methodology; writing – original draft. **Dominique Ferrandon:** Conceptualization; resources; supervision; funding acquisition; validation; methodology; writing – original draft; project administration; writing – review and editing.

Disclosure and competing interests statement

The authors declare that they have no conflict of interest.

References

Alarco AM, Marcil A, Chen J, Suter B, Thomas D, Whiteway M (2004) Immune-deficient *Drosophila melanogaster*: a model for the innate immune response to human fungal pathogens. *J Immunol* 172: 5622 – 5628

Apidianakis Y, Rahme LG, Heitman J, Ausubel FM, Calderwood SB, Mylonakis E (2004) Challenge of *Drosophila melanogaster* with *Cryptococcus neoformans* and role of the innate immune response. *Eukaryot Cell* 3: 413 – 419

Benmimoun B, Papastefanaki F, Perichon B, Segklia K, Roby N, Miriagou V, Schmitt C, Dramsi S, Matsas R, Speder P (2020) An original infection model identifies host lipoprotein import as a route for blood-brain barrier crossing. *Nat Commun* 11: 6106

Blango MG, Kniemeyer O, Brakhage AA (2019) Conidial surface proteins at the interface of fungal infections. *PLoS Pathog* 15: e1007939

Bongomin F, Gago S, Oladele RO, Denning DW (2017) Global and multi-national prevalence of fungal diseases-estimate precision. *J Fungi* 3: 57

Brown R, Priest E, Naglik JR, Richardson JP (2021) Fungal toxins and host immune responses. *Front Microbiol* 12: 643639

Chikina AS, Nadalin F, Maurin M, San-Roman M, Thomas-Bonafos T, Li XV, Lameiras S, Baulande S, Henri S, Malissen B *et al* (2020) Macrophages maintain epithelium integrity by limiting fungal product absorption. *Cell* 183: e416

Clemmons AW, Lindsay SA, Wasserman SA (2015) An effector peptide family required for *Drosophila* toll-mediated immunity. *PLoS Pathog* 11: e1004876

Cohen LB, Lindsay SA, Xu Y, Lin SJH, Wasserman SA (2020) The Daisho peptides mediate *Drosophila* defense against a subset of filamentous fungi. *Front Immunol* 11: 9

Cramer RA Jr, Gamcsik MP, Brooking RM, Najvar LK, Kirkpatrick WR, Patterson TF, Balibar CJ, Graybill JR, Perfect JR, Abraham SN *et al* (2006) Disruption of a nonribosomal peptide synthetase in *Aspergillus fumigatus* eliminates gliotoxin production. *Eukaryot Cell* 5: 972 – 980

da Silva Ferreira ME, Kress MR, Savoldi M, Goldman MH, Hartl A, Heinekamp T, Brakhage AA, Goldman GH (2006) The akuB(KU80) mutant deficient for nonhomologous end joining is a powerful tool for analyzing pathogenicity in *Aspergillus fumigatus*. *Eukaryot Cell* 5: 207 – 211

De Gregorio E, Spellman PT, Tzou P, Rubin GM, Lemaitre B (2002) The Toll and Imd pathways are the major regulators of the immune response in *Drosophila*. *EMBO J* 21: 2568 – 2579

Dudzic JP, Hanson MA, Iatsenko I, Kondo S, Lemaitre B (2019) More than black or white: melanization and toll share regulatory serine proteases in *Drosophila*. *Cell Rep* 27: e1053

Dunbar TL, Yan Z, Balla KM, Smelkinson MG, Troemel ER (2012) *C. elegans* detects pathogen-induced translational inhibition to activate immune signaling. *Cell Host Microbe* 11: 375 – 386

Duneau D, Ferdy JB, Revah J, Kondolf H, Ortiz GA, Lazzaro BP, Buchon N (2017) Stochastic variation in the initial phase of bacterial infection predicts the probability of survival in *D. melanogaster*. *Elife* 6: e28298

Fando JL, Alaba I, Escarmis C, Fernandez-Luna JL, Mendez E, Salinas M (1985) The mode of action of restrictocin and mitogillin on eukaryotic ribosomes. Inhibition of brain protein synthesis, cleavage and sequence of the ribosomal RNA fragment. *Eur J Biochem* 149: 29 – 34

Fehlbaum P, Bulet P, Michaut L, Lagueux M, Brockaert WF, Hétru C, Hoffmann JA (1995) Septic injury of *Drosophila* induces the synthesis of a potent antifungal peptide with sequence homology to plant antifungal peptides. *J Biol Chem* 269: 33159 – 33163

Ferrandon D (2013) The complementary facets of epithelial host defenses in the genetic model organism *Drosophila melanogaster*: from resistance to resilience. *Curr Opin Immunol* 25: 59 – 70

Ferreira AG, Naylor H, Esteves SS, Pais IS, Martins NE, Teixeira L (2014) The Toll-dorsal pathway is required for resistance to viral oral infection in *Drosophila*. *PLoS Pathog* 10: e1004507

Frisvad JC, Rank C, Nielsen KF, Larsen TO (2009) Metabolomics of *Aspergillus fumigatus*. *Med Mycol* 47: S53 – S71

Gago S, Denning DW, Bowyer P (2019) Pathophysiological aspects of *Aspergillus* colonization in disease. *Med Mycol* 57: S219 – S227

Gant DB, Cole RJ, Valdes JJ, Eldefrawi ME, Eldefrawi AT (1987) Action of tremorgenic mycotoxins on GABAA receptor. *Life Sci* 41: 2207 – 2214

Gao Q, Jin K, Ying SH, Zhang Y, Xiao G, Shang Y, Duan Z, Hu X, Xie XQ, Zhou G *et al* (2011) Genome sequencing and comparative transcriptomics of the model entomopathogenic fungi *Metarhizium anisopliae* and *M. acridum*. *PLoS Genet* 7: e1001264

Gluck A, Endo Y, Wool IG (1994) The ribosomal RNA identity elements for ricin and for alpha-sarcin: mutations in the putative CG pair that closes a GAGA tetraloop. *Nucleic Acids Res* 22: 321 – 324

Gottar M, Gobert V, Matskevich AA, Reichhart JM, Wang C, Butt TM, Belvin M, Hoffmann JA, Ferrandon D (2006) Dual detection of fungal infections in *Drosophila* via recognition of glucans and sensing of virulence factors. *Cell* 127: 1425 – 1437

Greaney AJ, Leppla SH, Moayeri M (2015) Bacterial exotoxins and the inflammasome. *Front Immunol* 6: 570

Gross L, Vicens Q, Einhorn E, Noireterre A, Schaeffer L, Kuhn L, Imler JL, Eriani G, Meignin C, Martin F (2017) The IRES 5′UTR of the dicistrovirus cricket paralysis virus is a type III IRES containing an essential pseudoknot structure. *Nucleic Acids Res* 45: 8993 – 9004

Hanson MA, Lemaitre B (2020) New insights on *Drosophila* antimicrobial peptide function in host defense and beyond. *Curr Opin Immunol* 62: 22 – 30

Hanson MA, Dostalova A, Ceroni C, Poidevin M, Kondo S, Lemaitre B (2019) Synergy and remarkable specificity of antimicrobial peptides *in vivo* using a systematic knockout approach. *Elife* 8: e44341

Hillmann F, Novohradska S, Mattern DJ, Forberger T, Heinekamp T, Westermann M, Winckler T, Brakhage AA (2015) Virulence determinants of the human pathogenic fungus *Aspergillus fumigatus* protect against soil amoeba predation. *Environ Microbiol* 17: 2858 – 2869

Hotujac L, Muftic RH, Filipovic N (1976) Verruculogen: a new substance for decreasing of GABA levels in CNS. *Pharmacology* 14: 297 – 300

Huang J, Lou Y, Liu J, Bulet P, Jiao R, Hoffmann JA, Liegeois S, Li Z, Ferrandon D (2022) A Toll pathway effector protects *Drosophila* specifically from distinct toxins secreted by a fungus or a bacterium. *bioRxiv* https://doi.org/10.1101/2020.11.23.394809 [PREPRINT]

Jahn B, Koch A, Schmidt A, Wanner G, Gehringer H, Bhakdi S, Brakhage AA (1997) Isolation and characterization of a pigmentless-conidium mutant of

© 2022 The Authors

14693178, 0, Downloaded from https://www.embopress.org/doi/10.15252/embr.202256036 by Cochrane France, Wiley Online Library on [02/12/2022]. See the Terms and Conditions (https://onlinelibrary.wiley.com/terms-and-conditions) on Wiley Online Library for rules of use; OA articles are governed by the applicable Creative Commons License

Aspergillus fumigatus with altered conidial surface and reduced virulence. *Infect Immun* 65: 5110 – 5117

Johns A, Scharf DH, Gsaller F, Schmidt H, Heinekamp T, Strassburger M, Oliver JD, Birch M, Beckmann N, Dobb KS *et al* (2017) A nonredundant phosphopantetheinyl transferase, PptA, is a novel antifungal target that directs secondary metabolite, siderophore, and lysine biosynthesis in *Aspergillus fumigatus* and is critical for pathogenicity. *mBio* 8: e01504-16

Kato N, Suzuki H, Okumura H, Takahashi S, Osada H (2013) A point mutation in ftmD blocks the fumitremorgin biosynthetic pathway in *Aspergillus fumigatus* strain Af293. *Biosci Biotechnol Biochem* 77: 1061 – 1067

Knaus HG, McManus OB, Lee SH, Schmalhofer WA, Garcia-Calvo M, Helms LM, Sanchez M, Giangiacomo K, Reuben JP, Smith AB 3rd *et al* (1994) Tremorgenic indole alkaloids potently inhibit smooth muscle high-conductance calcium-activated potassium channels. *Biochemistry* 33: 5819 – 5828

Konig S, Pace S, Pein H, Heinekamp T, Kramer J, Romp E, Strassburger M, Troisi F, Proschak A, Dworschak J *et al* (2019) Gliotoxin from *Aspergillus fumigatus* abrogates leukotriene B4 formation through inhibition of leukotriene A4 hydrolase. *Cell Chem Biol* 26: e525

Kosmidis C, Denning DW (2015) The clinical spectrum of pulmonary aspergillosis. *Thorax* 70: 270 – 277

Kubodera T, Yamashita N, Nishimura A (2000) Pyrithiamine resistance gene (ptrA) of *Aspergillus oryzae*: cloning, characterization and application as a dominant selectable marker for transformation. *Biosci Biotechnol Biochem* 64: 1416 – 1421

Kudryashova E, Quintyn R, Seveau S, Lu W, Wysocki VH, Kudryashov DS (2014) Human defensins facilitate local unfolding of thermodynamically unstable regions of bacterial protein toxins. *Immunity* 41: 709 – 721

Kupfahl C, Heinekamp T, Geginat G, Ruppert T, Hartl A, Hof H, Brakhage AA (2006) Deletion of the gliP gene of *Aspergillus fumigatus* results in loss of gliotoxin production but has no effect on virulence of the fungus in a low-dose mouse infection model. *Mol Microbiol* 62: 292 – 302

Lamy B, Moutaouakil M, Latge JP, Davies J (1991) Secretion of a potential virulence factor, a fungal ribonucleotoxin, during human aspergillosis infections. *Mol Microbiol* 5: 1811 – 1815

Lazzaro BP, Zasloff M, Rolff J (2020) Antimicrobial peptides: application informed by evolution. *Science* 368: eaau5480

Lebrigand K, He LD, Thakur N, Arguel MJ, Polanowska J, Henrissat B, Record E, Magdelenat G, Barbe V, Raffaele S *et al* (2016) Comparative genomic analysis of *Drechmeria coniospora* reveals Core and specific genetic requirements for fungal endoparasitism of nematodes. *PLoS Genet* 12: e1006017

Lee KZ, Lestradet M, Socha C, Schirmeier S, Schmitz A, Spenle C, Lefebvre O, Keime C, Yamba WM, Bou Aoun R *et al* (2016) Enterocyte purge and rapid recovery is a resilience reaction of the gut epithelium to pore-forming toxin attack. *Cell Host Microbe* 20: 716 – 730

Lemaitre B, Hoffmann J (2007) The host defense of *Drosophila melanogaster*. *Annu Rev Immunol* 25: 697 – 743

Lemaitre B, Nicolas E, Michaut L, Reichhart JM, Hoffmann JA (1996) The dorsoventral regulatory gene cassette *spätzle/Toll/cactus* controls the potent antifungal response in *Drosophila* adults. *Cell* 86: 973 – 983

Lesperance DN, Broderick NA (2020) Microbiomes as modulators of *Drosophila melanogaster* homeostasis and disease. *Curr Opin Insect Sci* 39: 84 – 90

Levashina EA, Ohresser S, Bulet P, Reichhart J-M, Hétru C, Hoffmann JA (1995) Metchnikowin, a novel immune-inducible proline-rich peptide from *Drosophila* with antibacterial and antifungal properties. *Eur J Biochem* 233: 694 – 700

Liegeois S, Ferrandon D (2022) Sensing microbial infections in the *Drosophila melanogaster* genetic model organism. *Immunogenetics* 74: 35 – 62

Lin SJH, Cohen LB, Wasserman SA (2020) Effector specificity and function in *Drosophila* innate immunity: getting AMPed and dropping Boms. *PLoS Pathog* 16: e1008480

Lindsay SA, Lin SJH, Wasserman SA (2018) Short-form Bomanins mediate humoral immunity in *Drosophila*. *J Innate Immun* 10: 306 – 314

Macheleidt J, Mattern DJ, Fischer J, Netzker T, Weber J, Schroeckh V, Valiante V, Brakhage AA (2016) Regulation and role of fungal secondary metabolites. *Annu Rev Genet* 50: 371 – 392

Madic J, Zocevic A, Senlis V, Fradet E, Andre B, Muller S, Dangla R, Droniou ME (2016) Three-color crystal digital PCR. *Biomol Detect Quantif* 10: 34 – 46

Martin F, Barends S, Jaeger S, Schaeffer L, Prongidi-Fix L, Eriani G (2011) Cap-assisted internal initiation of translation of histone H4. *Mol Cell* 41: 197 – 209

McEwan DL, Kirienko NV, Ausubel FM (2012) Host translational inhibition by *Pseudomonas aeruginosa* exotoxin A triggers an immune response in *Caenorhabditis elegans*. *Cell Host Microbe* 11: 364 – 374

Medzhitov R, Schneider DS, Soares MP (2012) Disease tolerance as a defense strategy. *Science* 335: 936 – 941

Melo JA, Ruvkun G (2012) Inactivation of conserved *C. elegans* genes engages pathogen- and xenobiotic-associated defenses. *Cell* 149: 452 – 466

Nam HJ, Jang IH, You H, Lee KA, Lee WJ (2012) Genetic evidence of a redox-dependent systemic wound response via Hayan protease-phenoloxidase system in *Drosophila*. *EMBO J* 31: 1253 – 1265

Nayak SK, Bagga S, Gaur D, Nair DT, Salunke DM, Batra JK (2001) Mechanism of specific target recognition and RNA hydrolysis by ribonucleolytic toxin restrictocin. *Biochemistry* 40: 9115 – 9124

Nehme NT, Quintin J, Cho JH, Lee J, Lafarge MC, Kocks C, Ferrandon D (2011) Relative roles of the cellular and humoral responses in the *Drosophila* host defense against three gram-positive bacterial infections. *PLoS One* 6: e14743

Norris PJ, Smith CC, De Belleroche J, Bradford HF, Mantle PG, Thomas AJ, Penny RH (1980) Actions of tremorgenic fungal toxins on neurotransmitter release. *J Neurochem* 34: 33 – 42

Pahl HL, Krauss B, Schulze-Osthoff K, Decker T, Traenckner EB, Vogt M, Myers C, Parks T, Warring P, Muhlbacher A *et al* (1996) The immunosuppressive fungal metabolite gliotoxin specifically inhibits transcription factor NF-kappaB. *J Exp Med* 183: 1829 – 1840

Quintin J, Asmar J, Matskevich AA, Lafarge MC, Ferrandon D (2013) The *Drosophila* Toll pathway controls but does not clear *Candida glabrata* infections. *J Immunol* 190: 2818 – 2827

Raffa N, Keller NP (2019) A call to arms: mustering secondary metabolites for success and survival of an opportunistic pathogen. *PLoS Pathog* 15: e1007606

Raisch T, Brockmann A, Ebbinghaus-Kintscher U, Freigang J, Gutbrod O, Kubicek J, Maertens B, Hofnagel O, Raunser S (2021) Small molecule modulation of the *Drosophila* Slo channel elucidated by cryo-EM. *Nat Commun* 12: 7164

Rodrigues ML, Nosanchuk JD (2020) Fungal diseases as neglected pathogens: a wake-up call to public health officials. *PLoS Negl Trop Dis* 14: e0007964

Scharf DH, Heinekamp T, Brakhage AA (2014) Human and plant fungal pathogens: the role of secondary metabolites. *PLoS Pathog* 10: e1003859

Soares MP, Teixeira L, Moita LF (2017) Disease tolerance and immunity in host protection against infection. *Nat Rev Immunol* 17: 83 – 96

 © 2022 The Authors

14693178, 0, Downloaded from https://www.embopress.org/doi/10.15252/embr.202256036 by Cochrane France, Wiley Online Library on [02/12/2022]. See the Terms and Conditions (https://onlinelibrary.wiley.com/terms-and-conditions) on Wiley Online Library for rules of use; OA articles are governed by the applicable Creative Commons License

Sun H, Towb P, Chiem DN, Foster BA, Wasserman SA (2004) Regulated assembly of the Toll signaling complex drives *Drosophila* dorsoventral patterning. *EMBO J* 23: 100 – 110

Szewczyk E, Nayak T, Oakley CE, Edgerton H, Xiong Y, Taheri-Talesh N, Osmani SA, Oakley BR (2006) Fusion PCR and gene targeting in *Aspergillus nidulans*. *Nat Protoc* 1: 3111 – 3120

Uttenweiler-Joseph S, Moniatte M, Lagueux M, Van Dorsselaer A, Hoffmann JA, Bulet P (1998) Differential display of peptides induced during the immune response of *Drosophila*: a matrix-assisted laser desorption ionization time-of-flight mass spectrometry study. *Proc Natl Acad Sci USA* 95: 11342 – 11347

van de Veerdonk FL, Gresnigt MS, Romani L, Netea MG, Latge JP (2017) *Aspergillus fumigatus* morphology and dynamic host interactions. *Nat Rev Microbiol* 15: 661 – 674

License: This is an open access article under the terms of the Creative Commons Attribution-NonCommercial-NoDerivs License, which permits use and distribution in any medium, provided the original work is properly cited, the use is non-commercial and no modifications or adaptations are made.

14693178, 0, Downloaded from https://www.embopress.org/doi/10.15252/embr.202256036 by Cochrane France, Wiley Online Library on [02/12/2022]. See the Terms and Conditions (https://onlinelibrary.wiley.com/terms-and-conditions) on Wiley Online Library for rules of use; OA articles are governed by the applicable Creative Commons License

Expanded View Figures

Figure EV1. *Aspergillus fumigatus* induces mortality in *MyD88* mutant flies (related to Fig 1).

A Survival of three different *Drosophila* wild-type strains to the injection of 50, 500, or 5,000 *A. fumigatus* conidia (20 flies per condition).
B Survival of hemizygous (HZ) *MyD88/Df(2R)3591* flies after the injection of 250 conidia of wild-type *A. fumigatus* conidia (20 flies per condition).
C Survival of wild-type and *MyD88* flies after the injection of 250 conidia from different wild-type *A. fumigatus* strains (error bars represent mean ± SD of the survival of biological triplicates of 20 flies each).
D, E Survival of the Toll pathway mutant flies, *spz* (D) and *Toll* (E) (20 flies per condition, 500 conidia per fly); the caption in (D) applies also to panel (E).
F Fungal load of single *MyD88* mutant and wild-type flies (biological replicates, 5,000 conidia injected per fly).
G Fungal load upon the death of single *MyD88* mutant flies (biological replicates).
H GFP-labeled *A. fumigatus* injected in wild-type flies form hyphae under a bright field (arrow shows the position of the blown-up area). The same preparation under fluorescence illumination is shown in Fig 1C. Scale bar 50 μm.
I 500 conidia of GFP-labeled *A. fumigatus* injected in *MyD88* mutant flies form few hyphae (arrow shows the position of the blown-up area) as compared to the injection of 50 conidia (shown in Fig 1E). Scale bar 50 μm.
J–L Survival of antibiotics-treated (J), axenic (K), and untreated flies (L) after injection of 250 *A. fumigatus* conidia (20 flies per condition).

Data Information: In (F, G), the middle bar of box plots represents the median and the upper and lower limits of boxes indicate, respectively, the first and third quartiles; the whiskers define the minima and maxima; data were analyzed using the Mann–Whitney statistical test. Survival curves were analyzed using the log-rank test.
****$P < 0.0001$, and NS: not significant.

© 2022 The Authors

14693178, 0, Downloaded from https://www.embopress.org/doi/10.15252/embr.202256036 by Cochrane France, Wiley Online Library on [02/12/2022]. See the Terms and Conditions (https://onlinelibrary.wiley.com/terms-and-conditions) on Wiley Online Library for rules of use; OA articles are governed by the applicable Creative Commons License

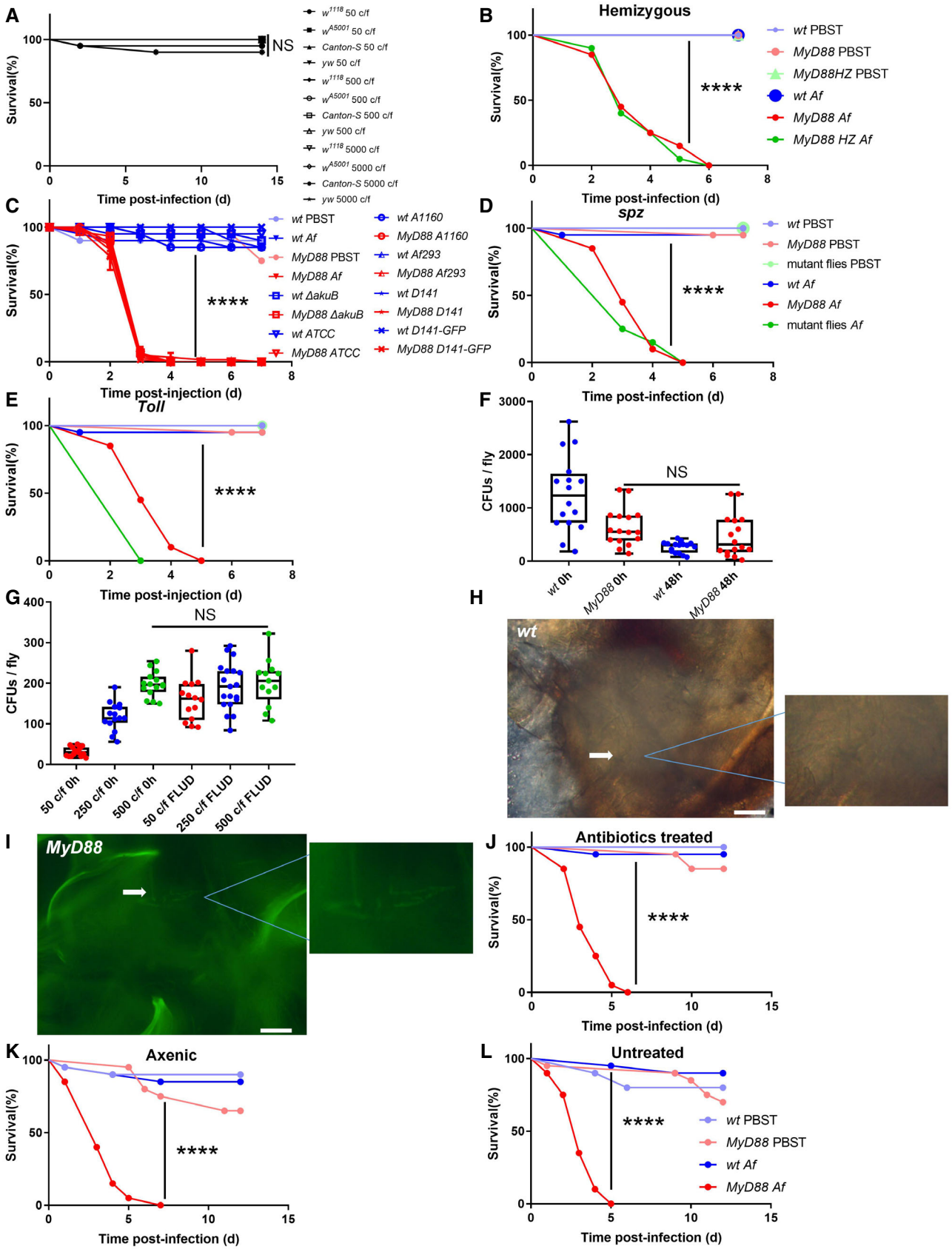


Figure EV1.

14693178, 0, Downloaded from https://www.embopress.org/doi/10.15252/embr.202256036 by Cochrane France, Wiley Online Library on [02/12/2022]. See the Terms and Conditions (https://onlinelibrary.wiley.com/terms-and-conditions) on Wiley Online Library for rules of use; OA articles are governed by the applicable Creative Commons License

Figure EV2. *55C* locus *Bomanins* are induced after *Aspergillus fumigatus* infection in a MyD88-dependent manner (related to Figs 1 and 5).

A Scheme of the 55C *Bomanin* locus.

B Expression level of *Bomanins* measured by RT–dPCR 48 h after *M. luteus* challenge (pooled data of $n = 3$ experiments, biological replicates).

C, D Expression levels of *Drosomycin* and *Bomanin S1* measured by RT–dPCR 48 h after challenge; *Drosomycin* $^*P = 0.03$; *BomS1*: $^*P = 0.03$ (pooled data of $n = 3$ experiments, biological replicates).

E, F MALDI-TOF mass spectrometry enlarged spectrum focused on BomS (E) or Drosomycin (F) of the hemolymph collected from an *A. fumigatus*-infected (5 conidia; green) or PBST-injected control (blue) fly.

G Peak intensity of short *Bomanins* and *Drosomycin* peptides post *A. fumigatus* injection. MALDI-TOF was used to measure the peptides in the hemolymph after the injection of different doses of conidia (*x*-axis) into wild-type flies. The same volume of PBS was injected into flies as a control.

Data Information: In (B–D), the middle bar of box plots represents the median and the upper and lower limits of boxes indicate, respectively, the first and third quartiles; the whiskers define the minima and maxima; data were analyzed using the Mann–Whitney statistical test. $^*P < 0.05$, and NS: not significant. (E–G) Hemolymph was collected at 48 h postinjection.

© 2022 The Authors

14693178, 0, Downloaded from https://www.embopress.org/doi/10.15252/embr.202256036 by Cochrane France, Wiley Online Library on [02/12/2022]. See the Terms and Conditions (https://onlinelibrary.wiley.com/terms-and-conditions) on Wiley Online Library for rules of use; OA articles are governed by the applicable Creative Commons License

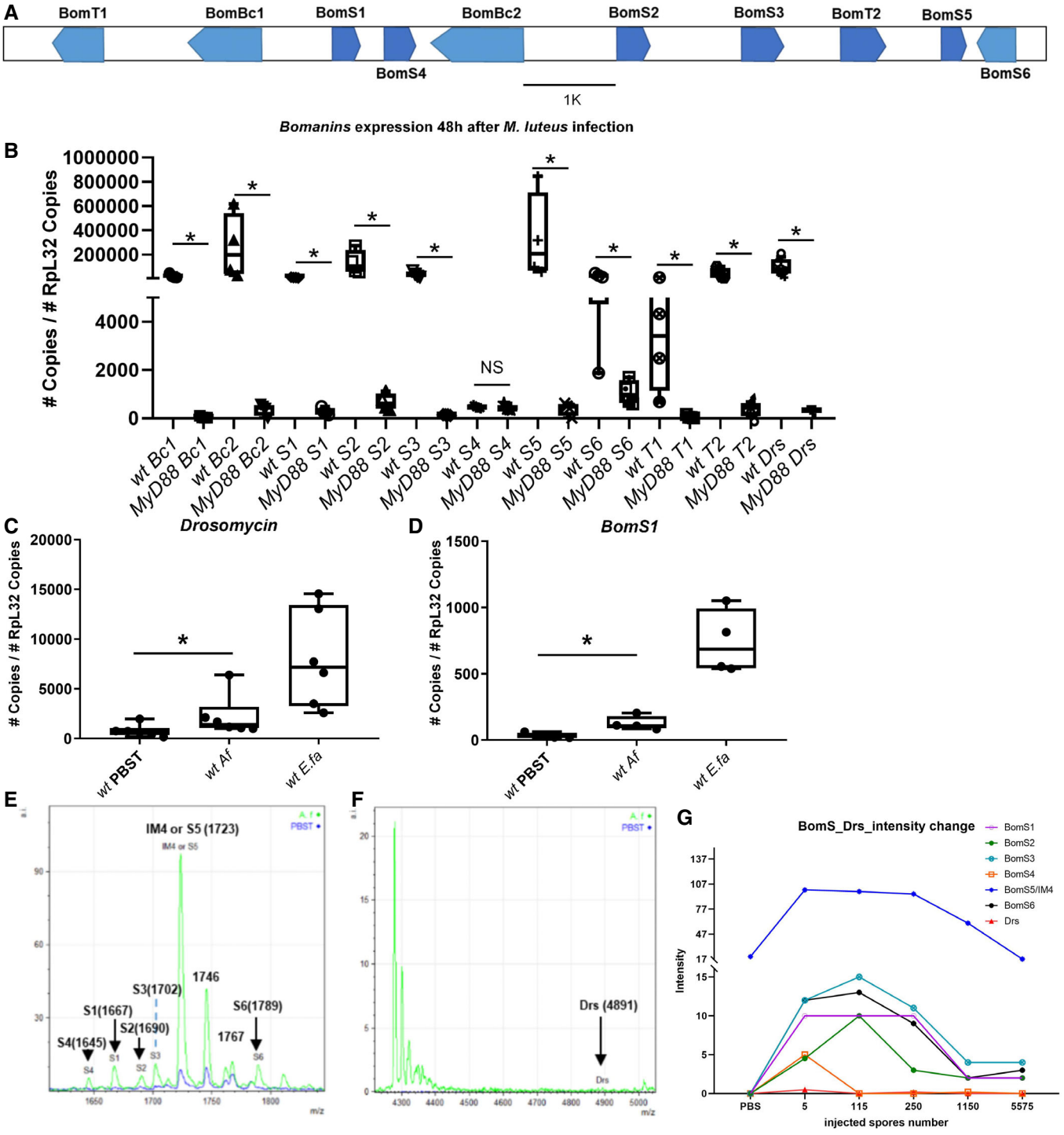


Figure EV2.

© 2022 The Authors

14693178, 0, Downloaded from https://www.embopress.org/doi/10.15252/embr.202256036 by Cochrane France, Wiley Online Library on [02/12/2022]. See the Terms and Conditions (https://onlinelibrary.wiley.com/terms-and-conditions) on Wiley Online Library for rules of use; OA articles are governed by the applicable Creative Commons License

Figure EV3. Role for specific melanization genes in host defense against *Aspergillus fumigatus* infection (related to Fig 1).

A, B Survival of *PPO1* (A) and *Sp7* mutant (B) flies injected with 500 *A. fumigatus* conidia.

C, D Survival (C) and fungal load upon death (D) of *PPO2* mutant flies after the injection of 500 *A. fumigatus* conidia ((C): error bars represent mean ± SD of the survival of biological triplicates of 20 flies each).

E Analysis of the distribution of GFP-labeled *A. fumigatus* inside live *Hayan* and *MyD88* flies; fluorescent hyphae (arrows) were observed in the head (42.5%, 17/40), thorax (100%, 40/40), and abdomen (95%, 38/40) in *Hayan* flies (arrows), whereas they were observed only in the thorax (50%, 50/100) and abdomen (1%, 1/100) of *MyD88* flies (arrows). Scale bars 50 μm.

F *Spätzle*, *Toll*, and *MyD88* mutants display hyphae extruding from the thoraces of cadavers after *A. fumigatus* infection; arrows mark hyphae. Scale bars 500 μm.

Data Information: In (D), the middle bar of box plots represents the median and the upper and lower limits of boxes indicate, respectively, the first and third quartiles; the whiskers define the minima and maxima; data were analyzed using the Mann–Whitney statistical test. Survival curves were analyzed using the log-rank test; ****$P < 0.0001$; NS: not significant.

© 2022 The Authors

14693178, 0, Downloaded from https://www.embopress.org/doi/10.15252/embr.202256036 by Cochrane France, Wiley Online Library on [02/12/2022]. See the Terms and Conditions (https://onlinelibrary.wiley.com/terms-and-conditions) on Wiley Online Library for rules of use; OA articles are governed by the applicable Creative Commons License

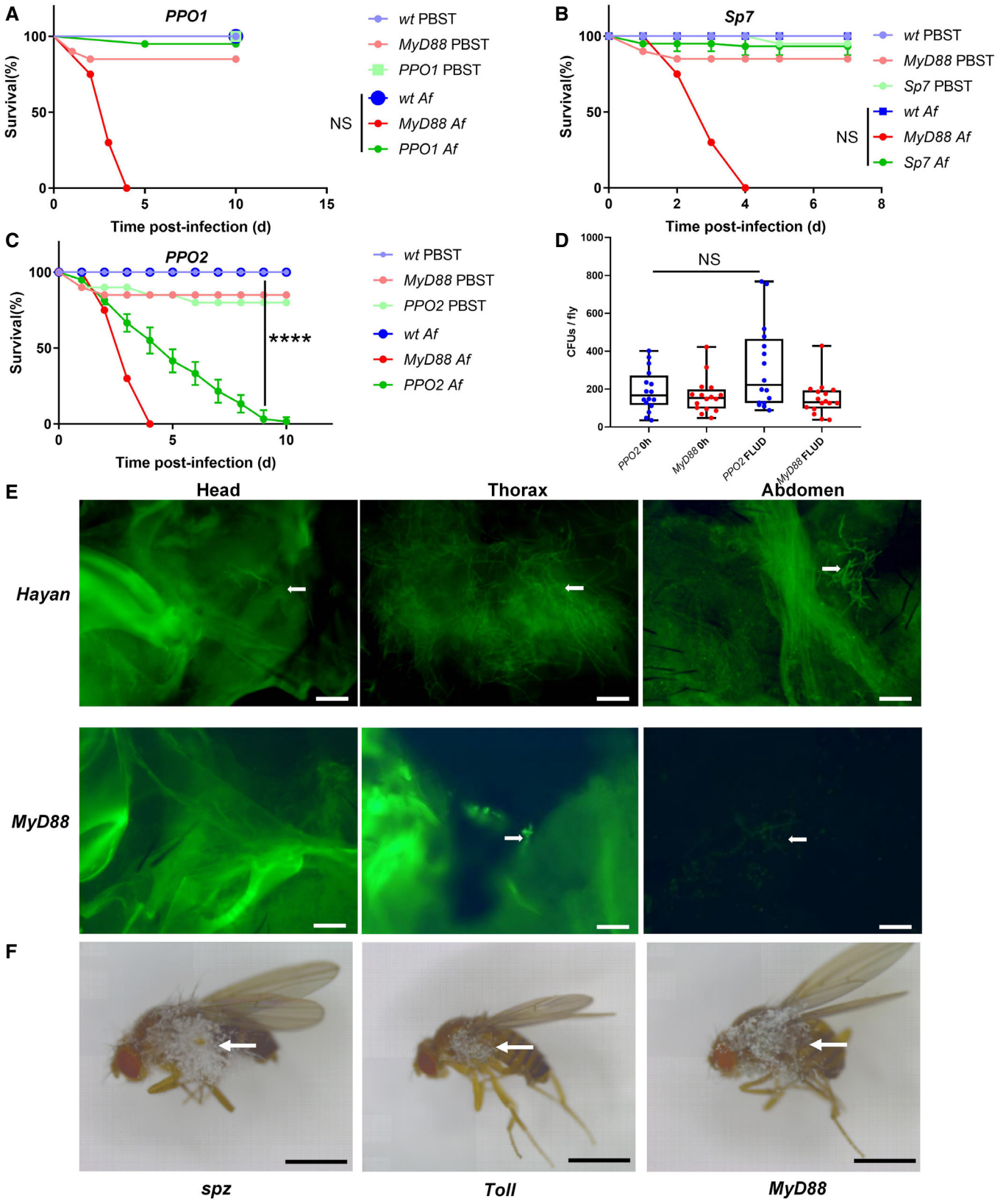


Figure EV3.

14693178, 0, Downloaded from https://www.embopress.org/doi/10.15252/embr.202256036 by Cochrane France, Wiley Online Library on [02/12/2022]. See the Terms and Conditions (https://onlinelibrary.wiley.com/terms-and-conditions) on Wiley Online Library for rules of use; OA articles are governed by the applicable Creative Commons License

Figure EV4. The Toll pathway is involved in the host defense against verruculogen and restrictocin but not melanization nor the cellular immune response (related to Figs 3 and 4).

A Survival of antibiotics-treated *MyD88* mutant flies after verruculogen solution injection.

B–G (B, C, F, G) Survival of *spätzle*, *Toll*, *Hayan*, and *PPO2* mutant flies after verruculogen injection; there was a significant difference between the treated and the vehicle control in *spätzle* (*$P = 0.01$; (B)) and *Toll* (****$P < 0.0001$ (C)) but not for *Hayan* or *PPO2* mutant flies (20 flies per condition). The caption for (G) applies to all four panels. (D) Recovery time from tremors in wild-type flies: each dot represents the time point of recovery of a single fly. Most *MyD88* flies did not recover (pooled data of $n = 3$ experiments, biological replicates). (E) Recovery time from tremors in $Bom^{\Delta 55C}$ mutant flies after verruculogen powder challenge (pooled data of $n = 3$ experiments, biological replicates).

H Survival of phago-hemoless *hml-Gal4-Gal80^{ts}* > UAS-*rpr*, UAS-*Hid* flies after verruculogen injection; there was no significant difference between the 29°C condition and the 18°C control for which there is no hemocyte ablation since Gal4 function is inhibited by the active Gal80 repressor (20 flies per condition).

I–L Survival of *spätzle* (I), *Toll* (J), *Hayan* (K), and *PPO2* (L) mutant flies after verruculogen injection; there is a significant difference between the treated and the vehicle control in *spätzle* and *Toll* (****$P < 0.0001$) but not for *Hayan* or *PPO2* mutant flies. The caption to the right of (L) applies to all four panels (20 flies per condition).

M Survival of phago-hemoless *hml-Gal4-Gal80^{ts}* > UAS-*rpr*, UAS-*Hid* flies after restrictocin injection; there is no significant difference between the 29°C condition and the 18°C control for which there is no hemocyte ablation since Gal4 is repressed (20 flies per condition).

Data Information: In (D, E), the middle bar of box plots represents the median and the upper and lower limits of boxes indicate, respectively, the first and third quartiles; the whiskers define the minima and maxima. Survival curves were analyzed using the log-rank test. (E) Data were analyzed using the Kruskal–Wallis test and Dunn's *post hoc* test. ****$P < 0.0001$, NS: not significant. The concentration of injected verruculogen or restrictocin was 1 mg/ml.

© 2022 The Authors

14693178, 0, Downloaded from https://www.embopress.org/doi/10.15252/embr.202256036 by Cochrane France, Wiley Online Library on [02/12/2022]. See the Terms and Conditions (https://onlinelibrary.wiley.com/terms-and-conditions) on Wiley Online Library for rules of use; OA articles are governed by the applicable Creative Commons License

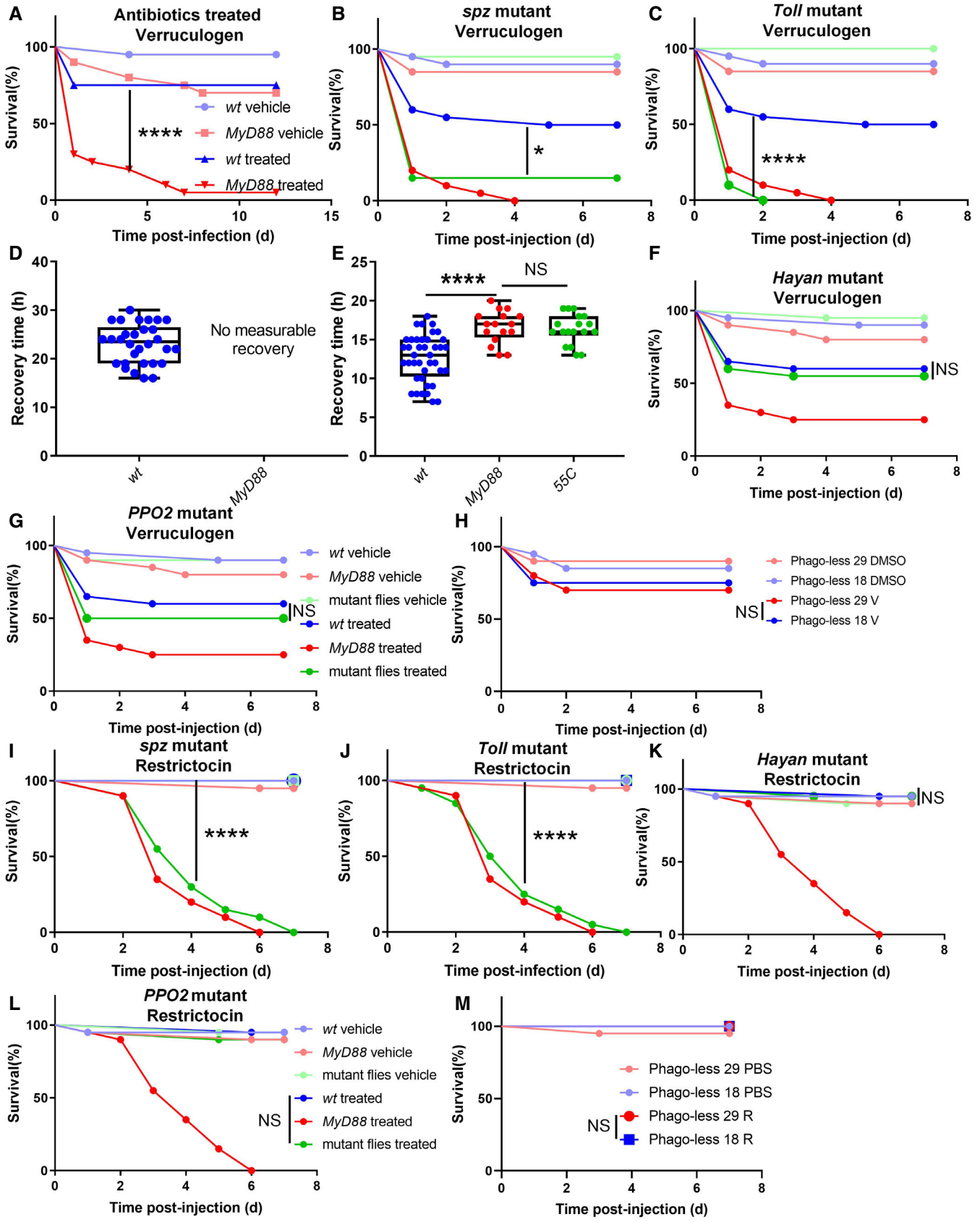


Figure EV4.

14693178, 0, Downloaded from https://www.embopress.org/doi/10.15252/embr.202256036 by Cochrane France, Wiley Online Library on [02/12/2022]. See the Terms and Conditions (https://onlinelibrary.wiley.com/terms-and-conditions) on Wiley Online Library for rules of use; OA articles are governed by the applicable Creative Commons License

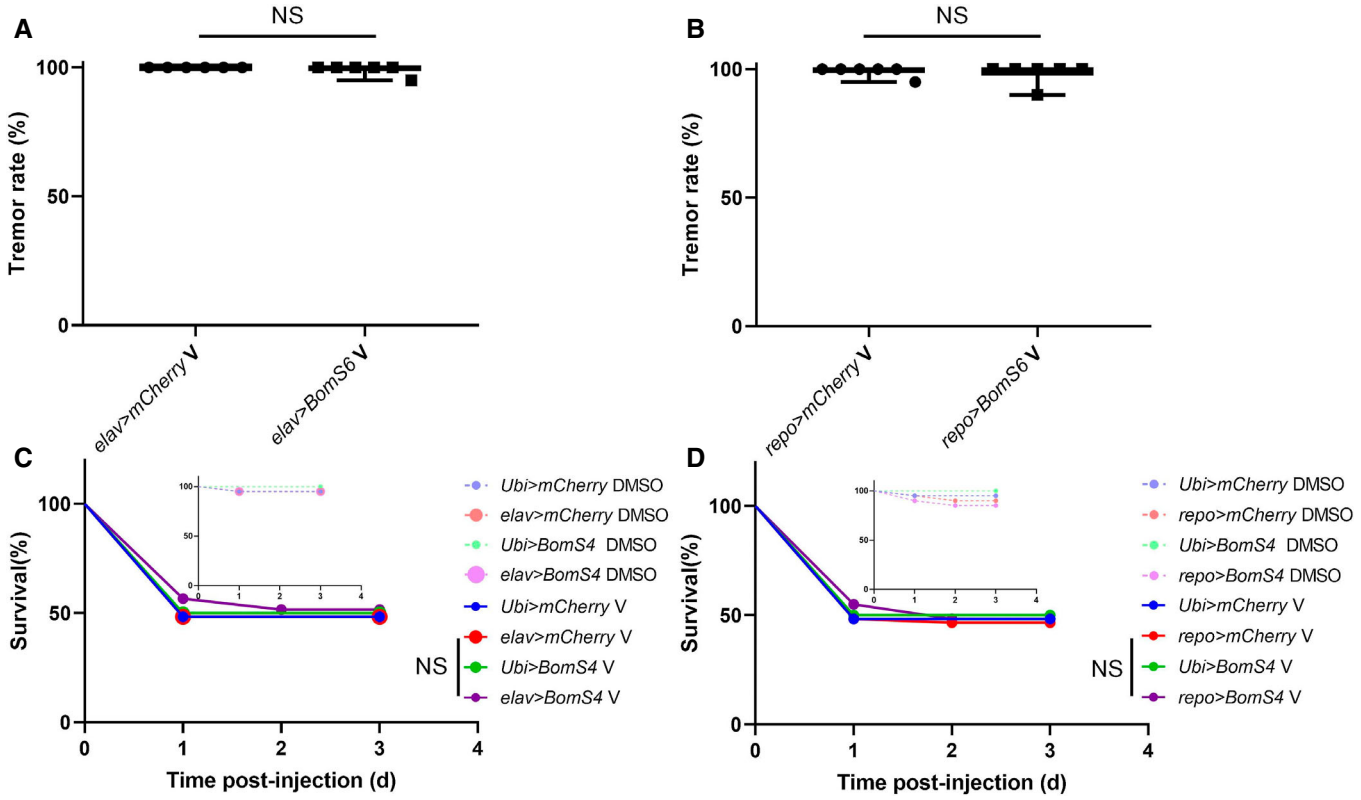


Figure EV5. BomS6 forced expression in the nervous system does not protect flies from early tremors induced by verruculogen injection (related to Fig 6).

A, B Tremor rate of *BomS6* overexpressed in neurons (A) or glia (B) flies (20 flies per condition, pooled data from $n = 3$ experiments, biological replicates) compared with wild-type after injection of verruculogen.

C, D Survival of *BomS4* overexpressed in neurons (C) or glia (D) flies (20 flies per condition) compared with wild-type 3 h after the injection of verruculogen. Insets represent the survival of vehicle control groups.

Data Information: In (A, B), the middle bar of box plots represents the median and the upper and lower limits of boxes indicate, respectively, the first and third quartiles; the whiskers define the minima and maxima; data were analyzed using the Mann–Whitney statistical test. Survival curves were analyzed using the log-rank test. The concentration of injected verruculogen was 1 mg/ml.

© 2022 The Authors

14693178, 0, Downloaded from https://www.embopress.org/doi/10.15252/embr.202256036 by Cochrane France, Wiley Online Library on [02/12/2022]. See the Terms and Conditions (https://onlinelibrary.wiley.com/terms-and-conditions) on Wiley Online Library for rules of use; OA articles are governed by the applicable Creative Commons License

The Toll pathway mediates *Drosophila* resilience to *Aspergillus* mycotoxins through specific Bomanins

Rui Xu, Yanyan Lou, Antonin Tidu, Philippe Bulet, Thorsten Heinekamp, Franck Martin, Axel Brakhage, Zi Li, Samuel Liégeois*, and Dominique Ferrandon[1-3]*

Table of Contents

Appendix Figure S1 -- page 2

Appendix Figure S2 -- page 3

Appendix Figure S3 -- page 4

Appendix Figure S4 -- page 5

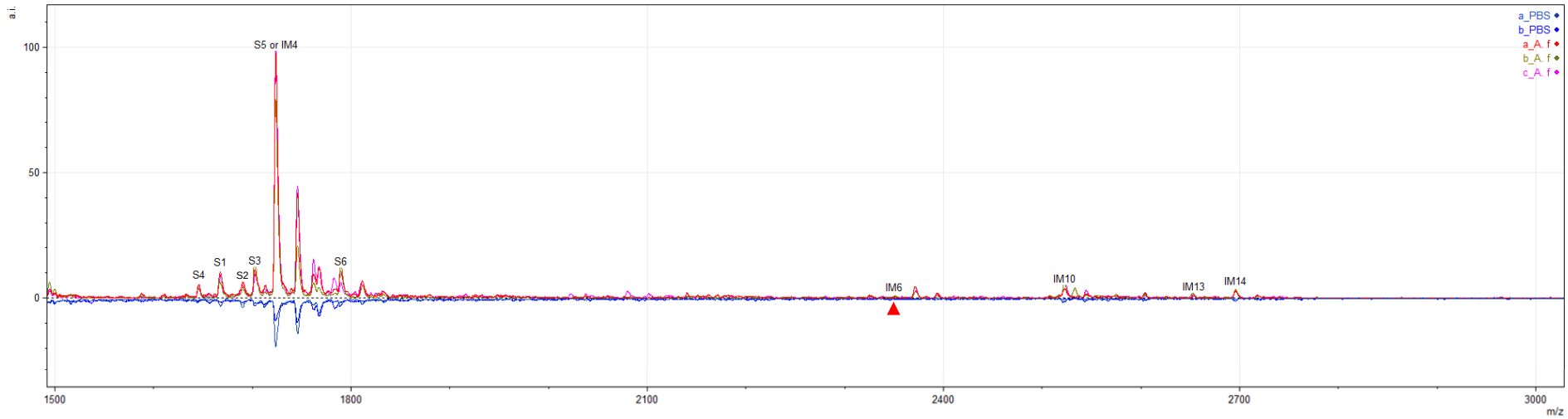
Appendix Figure S5 -- page 6

Appendix Figure S6 -- page 7

Appendix Figure S7 -- page 8

Appendix Table S1 -- page 9

14693178, 0, Downloaded from https://www.embopress.org/doi/10.15252/embr.202256036 by Cochrane France, Wiley Online Library on [02/12/2022]. See the Terms and Conditions (https://onlinelibrary.wiley.com/terms-and-conditions) on Wiley Online Library for rules of use; OA articles are governed by the applicable Creative Commons License

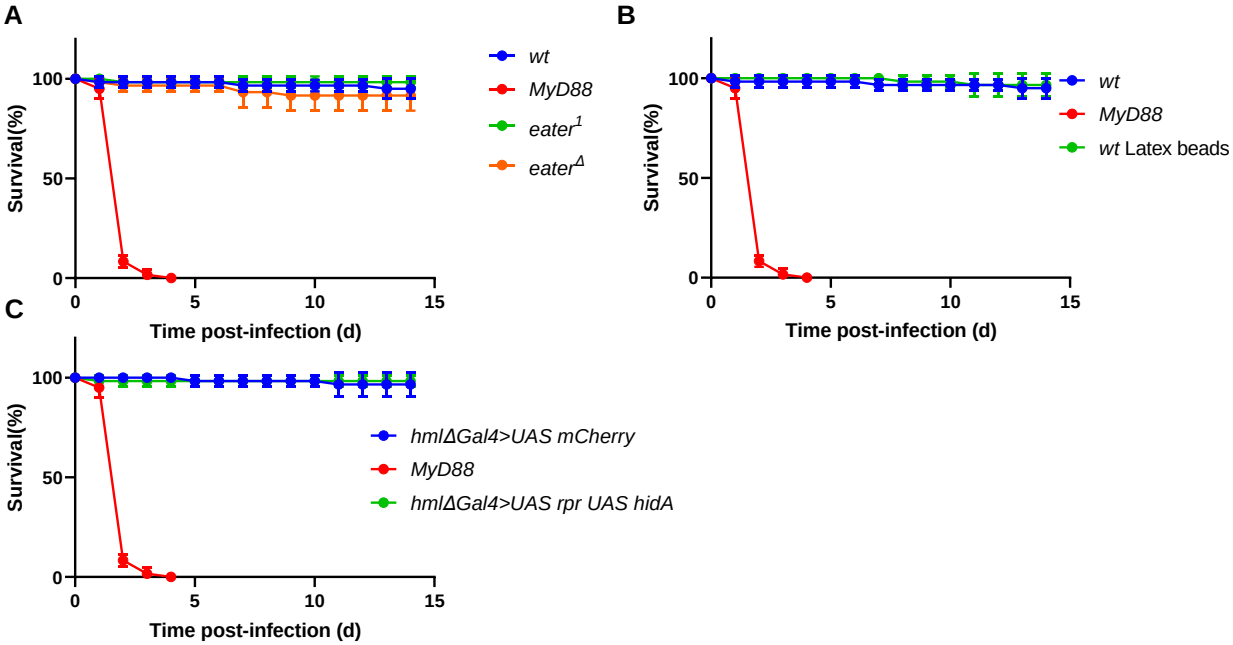


Appendix Figure S1. MALDI-TOF results after *A. fumigatus* challenge

Complementary to Fig. EV2.

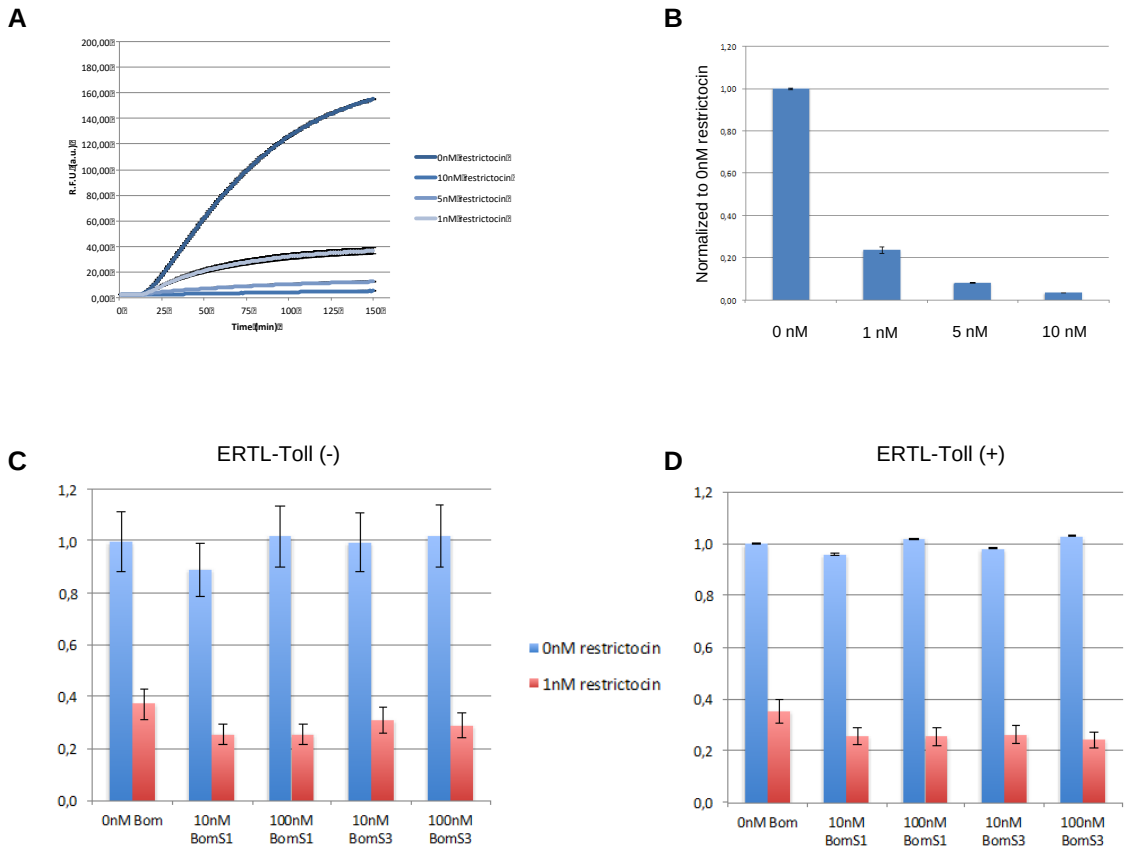
The hemolymph was collected at 48h post-injection of PBS or live spores. The blue lines under the 0 line of the x-axis (baseline) correspond to two PBS negative controls. The three curves above correspond to the signals gained on the hemolymph of three flies challenged with *A. fumigatus* live spores. All the Bomanin peptides were induced post *A. fumigatus* challenge but hardly after PBS injection. A few BaraA-derived peptides, IM10 and IM13 have been slightly induced. Furthermore, Daisho2 (IM14) is mildly expressed at this time point.

14693178, 0, Downloaded from https://www.embopress.org/doi/10.15252/emtr.202250936 by Cochrane France, Wiley Online Library on [02/12/2022]. See the Terms and Conditions (https://onlinelibrary.wiley.com/terms-and-conditions) on Wiley Online Library for rules of use; OA articles are governed by the applicable Creative Commons License



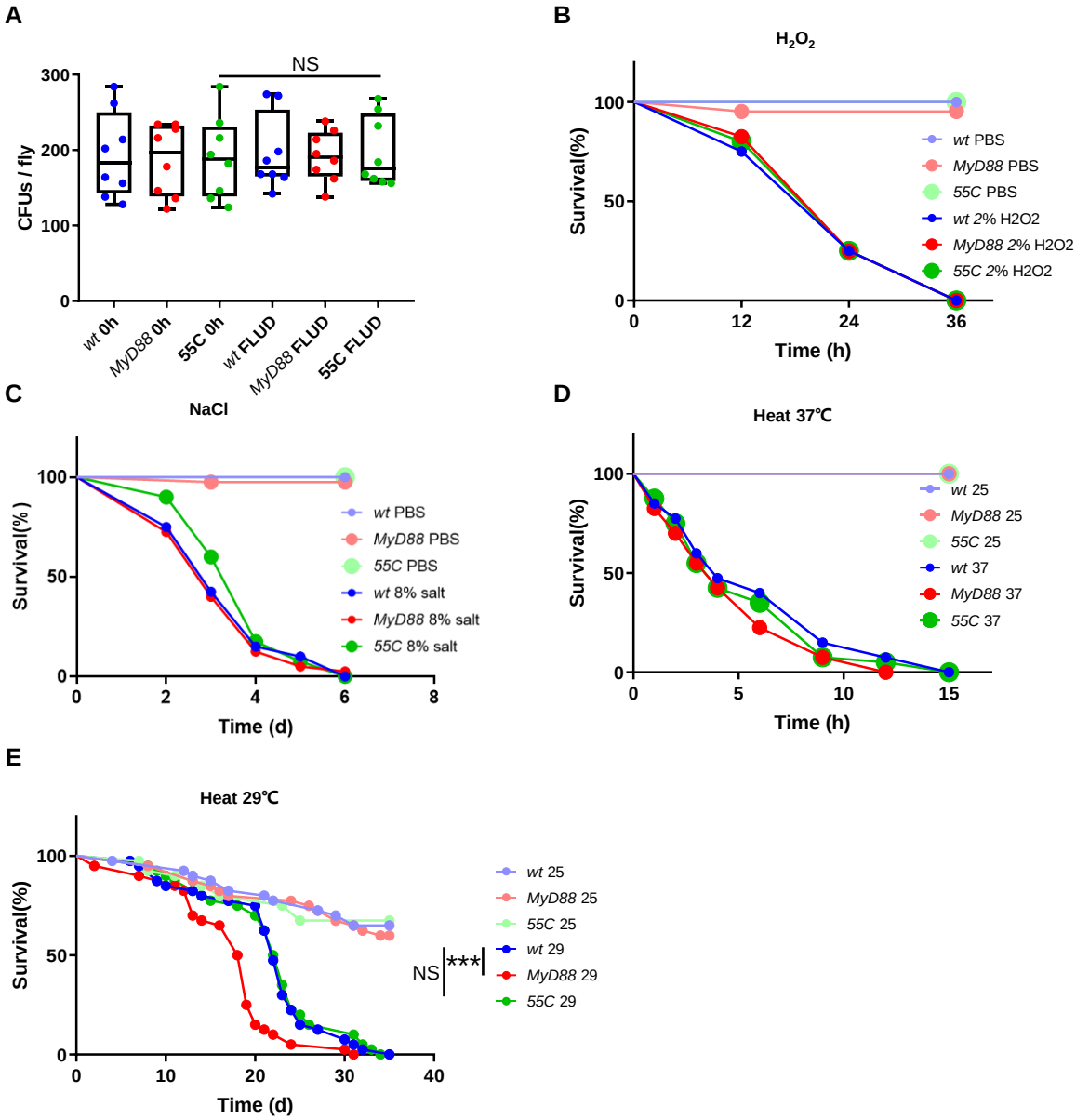
Appendix Figure S2. The cellular immune response is not involved in host defense against *A. fumigatus* infection.
Complementary to Fig. 1.
(*A*-*C*) survival of *eater* mutants, latex beads-treated, and phago-hemoless UAS-*rpr*, UAS-*Hid* flies (ablation of hemocytes) injected with 500 *A. fumigatus* conidia (*n*=60).
Data Information: survival curves were analyzed using the LogRank test

14693178, 0, Downloaded from https://www.embopress.org/doi/10.15252/embr.202256036 by Cochrane France, Wiley Online Library on [02/12/2022]. See the Terms and Conditions (https://onlinelibrary.wiley.com/terms-and-conditions) on Wiley Online Library for rules of use; OA articles are governed by the applicable Creative Commons License



Appendix Figure S3. Restrictocin inhibits *in vitro* translation even in the presence of BomS3.
Complementary to Fig. 4&5.
(*A-B*) translation kinetics analyzed by fluorescence measurements emitted by *in vitro* synthesized eGFP from an IGR(CrPV)-driven reporter in non-induced ERTL lysates: translation kinetics were depicted as the fluorescence emitted by *in vitro* synthetized eGFP in the presence of increasing concentrations of restrictocin (*A*) and by histogram representing the end-point fluorescence quantification of *A* (*B*). (*C-D*) histograms representing the end-point quantification of *in vitro* translated eGFP from an IGR(CrPV)-driven reporter in the absence or presence of 1 nM restrictocin, pre-incubated or not with either 10 or 100 nM BomS1 or BomS3 synthetic peptides using either noninduced ERTL lysates (*C*) or Toll-induced ERTL lysates (*D*).
Data Information: error bars represent the standard error of the mean from three technical replicates.

14693178, 0, Downloaded from https://www.embopress.org/doi/10.15252/embr.202256036 by Cochrane France, Wiley Online Library on [02/12/2022]. See the Terms and Conditions (https://onlinelibrary.wiley.com/terms-and-conditions) on Wiley Online Library for rules of use; OA articles are governed by the applicable Creative Commons License



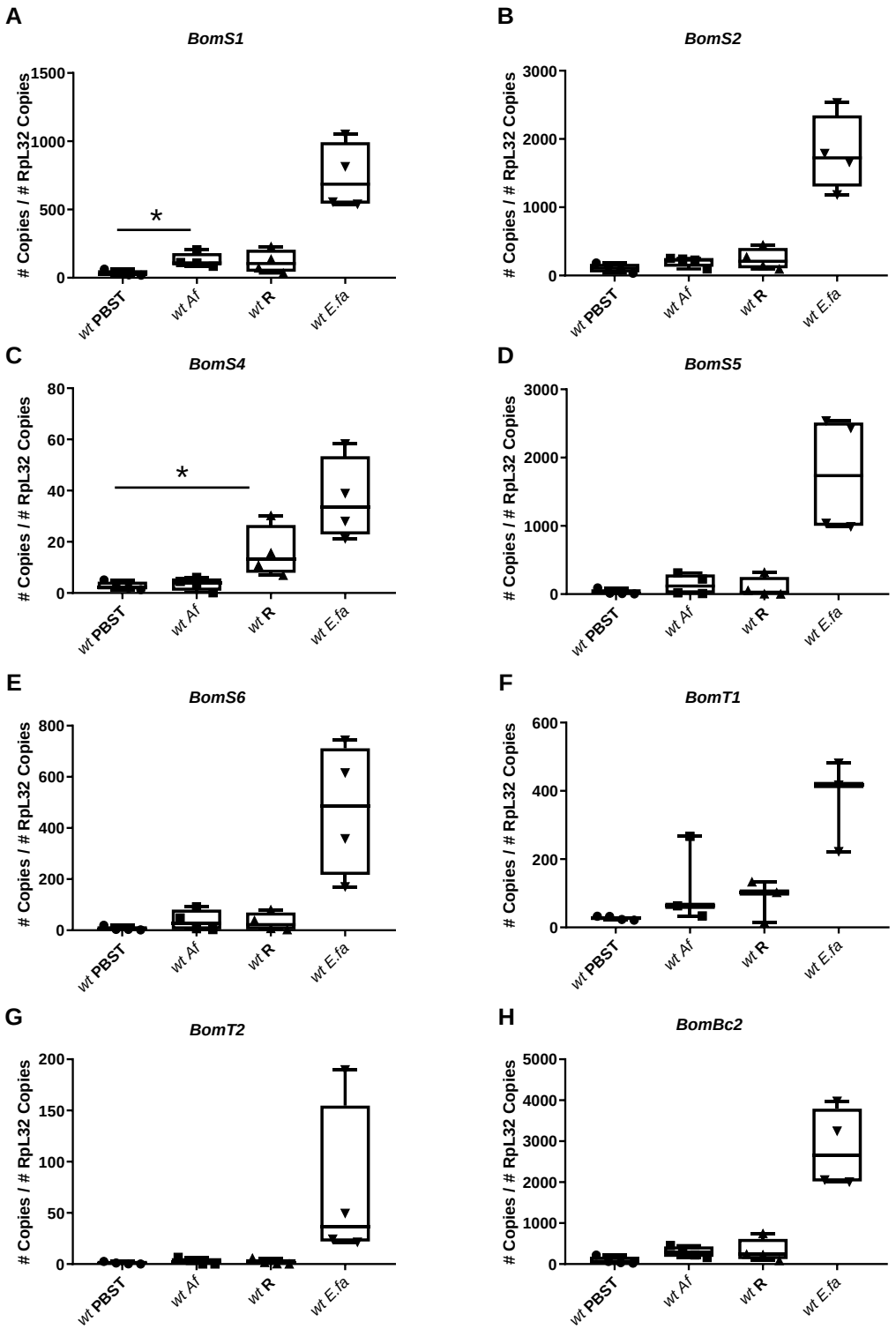
Appendix Figure S4. *Bom$^{\Delta 55C}$* mutant flies do not get an increased susceptibility to stress.

Complementary to Fig. 5.

(*A*) fungal load upon death of single *Bom$^{\Delta 55C}$* mutant flies. (*B-C*) survival of *Bom$^{\Delta 55C}$* (55C) deficient flies after H_2O_2 (*B*) or salt (*C*) solution injection; there was no significant difference between the treated and the 55C and wild-type treated groups (n=40). After H_2O_2 solution injection (*B*), wt *vs.* 55C, p=0.80; salt solution (*C*), wt *vs.* 55C, p=0.87. (*D-E*) survival of *Bom$^{\Delta 55C}$* (55C) deficient flies after 37°C (*D*) or 29°C (*E*) exposure; there was no significant difference between the 55C and wild-type treated groups, except the wild-type and *MyD88* treated groups exposed in 29°C (n=40). After exposition to 37°C (*D*), wt *vs.* 55C, p=0.51, wt *vs. MyD88*, p=0.012; 29°C (*E*), wt *vs.* 55C, p=0.75, wt *vs. MyD88*, p=0.0001.

Data Information: survival curves were analyzed using the LogRank test. NS: not significant.

14693178, 0, Downloaded from https://www.embopress.org/doi/10.15252/embr.202256036 by Cochrane France, Wiley Online Library on [02/12/2022]. See the Terms and Conditions (https://onlinelibrary.wiley.com/terms-and-conditions) on Wiley Online Library for rules of use; OA articles are governed by the applicable Creative Commons License



Appendix Figure S5. Expression level of *Bomanins* after *A. fumigatus* and mycotoxin challenge.

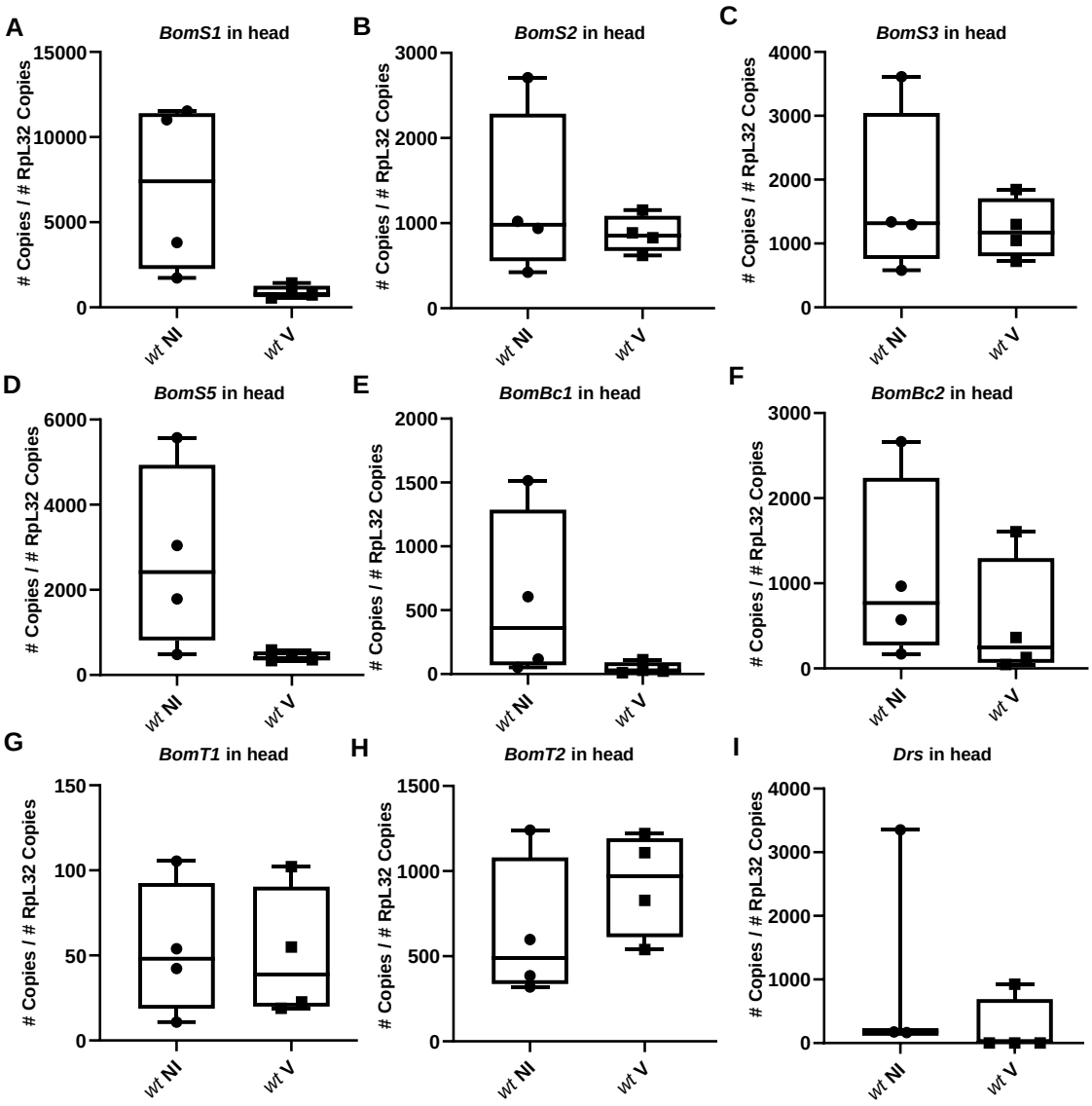
Complementary to Fig. 5.

(*A-G*) expression levels of *Bomanin* genes measured by RT-digital PCR 48 hours after challenge; except for *BomS4* (p=0.03), there was no significant difference between restrictocin and vehicle control injection for all *Bomanins*; except for *BomS1* (p=0.03), there was no significant difference between *A. fumigatus* and PBST control injection for all *Bomanins*.

Data Information: the middle bar of box plots represents the median and the upper and lower limits of boxes indicate respectively the first and third quartiles; the whiskers define the minima and maxima; data were analyzed using the Mann-Whitney statistical test.

The concentration of injected restrictocin was 1 mg/mL, the dose of *A. fumigatus* was 500 conidia per fly, *Enterococcus faecalis* infection was made by septic injury.

14693178, 0, Downloaded from https://www.embopress.org/doi/10.15252/embr.202256036 by Cochrane France, Wiley Online Library on [02/12/2022]. See the Terms and Conditions (https://onlinelibrary.wiley.com/terms-and-conditions) on Wiley Online Library for rules of use; OA articles are governed by the applicable Creative Commons License



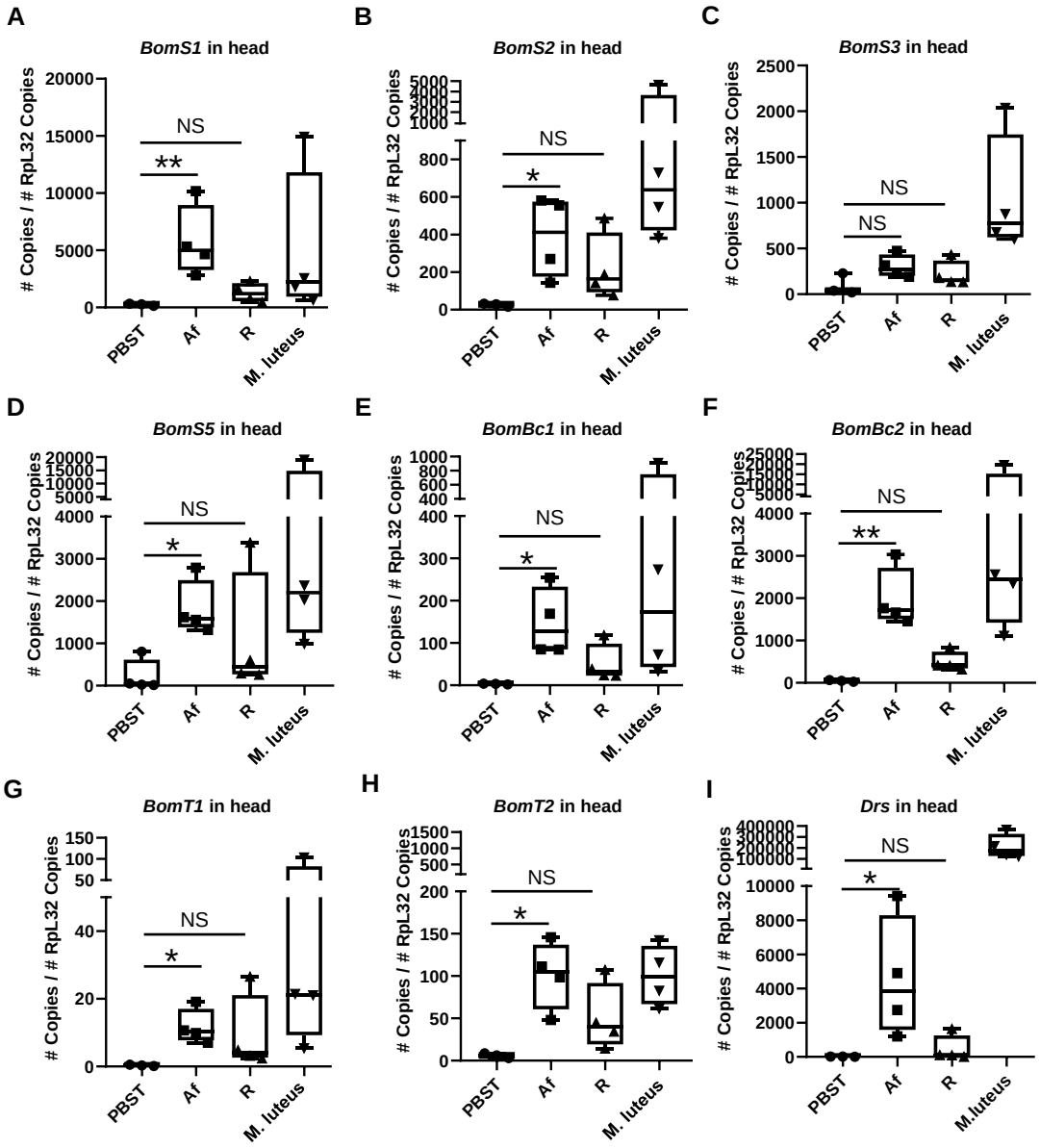
Appendix Figure S6. Expression level of *Bomanins* in the head after verruculogen challenge.

Complementary to Fig. 6.

(*A-I*) expression levels of *Bomanin* genes and *Drosomycin* measured by RT-digital PCR 48 hours after verruculogen powder challenge; there was no significant difference between verruculogen powder and blank control (NI) challenge.

Data Information: the middle bar of box plots represents the median and the upper and lower limits of boxes indicate respectively the first and third quartiles; the whiskers define the minima and maxima; data were analyzed using the Mann-Whitney statistical test.

14693178, 0, Downloaded from https://www.embopress.org/doi/10.15252/embr.202256036 by Cochrane France, Wiley Online Library on [02/12/2022]. See the Terms and Conditions (https://onlinelibrary.wiley.com/terms-and-conditions) on Wiley Online Library for rules of use; OA articles are governed by the applicable Creative Commons License



Appendix Figure S7. Expression level of *Bomanins* in head after *A. fumigatus* or restrictocin challenge.

Complementary to Fig. 6.

(*A-I*) expression levels of *Bomanin* genes and *Drosomycin* measured by RT-digital PCR 48 hours after challenge; except for *BomS3*, there were significant differences in *Bomanin* expression between *A. fumigatus* and vehicle control injection; there was no significant difference for *Bomanin* expression between restrictocin and PBST control injection.

Data Information: the middle bar of box plots represents the median and the upper and lower limits of boxes indicate respectively the first and third quartiles; the whiskers define the minima and maxima; data were analyzed using the Mann-Whitney statistical test. *$p < 0.05$, **$p < 0.01$, and NS: not significant.

The concentration of injected restrictocin was 1 mg/ml, the dose of *A. fumigatus* was 500 conidia per fly, *Micrococcus luteus* infection was made by septic injury.

14693178, 0, Downloaded from https://www.embopress.org/doi/10.15252/embr.202256036 by Cochrane France, Wiley Online Library on [02/12/2022]. See the Terms and Conditions (https://onlinelibrary.wiley.com/terms-and-conditions) on Wiley Online Library for rules of use; OA articles are governed by the applicable Creative Commons License

Appendix Table S1. Primers used in this study

RpL32	FW	GACGCTTCAAGGGACAGTATCTG
RpL32	RV	AAACGCGGTTCTGCATGAG
RpL32	Probe	**Cy5**-CATCGGTTACGGATCGAACA-**MGB**
Drosomycin	FW	CGTGAGAACCTTTTCCAATATGATG
Drosomycin	RV	TCCCAGGACCACCAGCAT
Drosomycin	Probe	**VIC**-AGATCAAGTACTTGTTCG-**MGB**
BomaninBc1	FW	TTTCGTTGTCCTGGCTTCCC
BomaninBc1	RV	CCGACTACGACGTTTTCCGC
BomaninBc1	Probe	**Cy5**-CTACGGCCGGAAATGTGAT-**MGB**
BomaninBc2	FW	AGAGCCTGACGTTATTGGCG
BomaninBc2	RV	TGGGAGCAGTTTACGCACTT
BomaninBc2	Probe	**FAM**-TGATCTTGGCCACGTTGGCCT-**MGB**
BomaninS1	FW	CAATGCTGTTCCACTGTCGC
BomaninS1	RV	CGTGGACATTGCACACCCTG
BomaninS1	Probe	**FAM**-ATCCAGGAAATGTGATCA-**MGB**
BomaninS2	FW	AGTCGTCACCGTCTTTGTGTT
BomaninS2	RV	CAGTATTTGCAGTCCCCGTTG
BomaninS2	Probe	**FAM**-CTGCTGGCTCTGGCCAAC-**MGB**
BomaninS3	FW	TCACTCGCCTTCGTTTTGGG
BomaninS3	RV	TTAGGCCCTCACATTGCAGAC
BomaninS3	Probe	**FAM**-GCTCTGGCCAACGCCACTC-**MGB**
BomaninS4	FW	GTTGTCACCCGATCCAGGAA
BomaninS4	RV	ATTTGCCACCACGAACATTGC
BomaninS4	Probe	**VIC**-TTATCATCAATGGCGACTG-**MGB**
BomaninS5	FW	GGTCTTTCTATGCGGTCTGCT
BomaninS5	RV	TAGCCTCCGCGAACATTACA
BomaninS5	Probe	**VIC**-CATGGCAGTGGCTTCTCCGTTA-**MGB**
BomaninS6	FW	GCTAGTGCCAATCCCCTGAG
BomaninS6	RV	TCGCCGCGTATATTGCAAAC
BomaninS6	Probe	**VIC**-CTGGCAATGTGATTATAAACG-**MGB**
BomaninT1	FW	TCCCAGGATTACCATTCGCA
BomaninT1	RV	GAGTTTTTGGTGGCGCGTG
BomaninT1	Probe	**Cy5**-CGACATTATAGTTCATGGCAAT-**MGB**
BomaninT2	FW	TAATGCTACGCCGGGACAAG
BomaninT2	RV	ATGGCTCCAGATGTGAGTGTG
BomaninT2	Probe	**Cy5**-ATGCATTGACTGCAATAAGCC-**MGB**
aspf1_up	FW	GAGATGGTGACTGCCTTTCC
aspf1_ptrA	RV	GGCCTGAGTGGCCATCGAATTCTCCAGGACATGGGATTGTCG
aspf1_ptrA	FW	GAGGCCATCTAGGCCATCAAGCCGTTGCTGCCACTCCTTTC
aspf1_dw	RV	ATTTCCACCCGTCTGTCCAG
ftmA_up	FW	GATTGGTTCTCCACTCTCGC
ftmA_ptrA	RV	GAGGCCATCTAGGCCATCAAGCCCATCGCCATAGTACAGACG
ftmA_ptrA	FW	GGCCTGAGTGGCCATCGAATTCGTCTGGATCGGTTCGACACC
ftmA_dw	RV	GACTTGGACAGAGGCTATAG
ptrA	FW	GAATTCGATGGCCACTCAGGCC
ptrA	RV	GCTTGATGGCTTAGATGGCCTC

14693178, 0, Downloaded from https://www.embopress.org/doi/10.15252/embr.202256036 by Cochrane France, Wiley Online Library on [02/12/2022]. See the Terms and Conditions (https://onlinelibrary.wiley.com/terms-and-conditions) on Wiley Online Library for rules of use; OA articles are governed by the applicable Creative Commons License